BSC

Design Calculation or Analysis Cover Sheet

Complete only applicable items.

1. QA: N/A

2. Page 1

3. System	4. Document Identifier
DOE and Commercial Waste Package	CAL-DS0-NU-000005 Rev 0B

5. Title

Criticality Potential of Waste Packages Affected by Igneous Intrusion

6. Group

Licensing & Nuclear Safety/Criticality

7. Document Status Designation

☐ Preliminary   ☒ Committed   ☐ Confirmed   ☐ Cancelled

8. Notes/Comments

This calculation was initiated by Darby Kimball and completed by Charlotta E. Sanders.

The calculations contained in this document were developed by Bechtel SAIC Company, LLC (BSC) and are intended solely for the use of BSC in its work for the Yucca Mountain Project.

Initial checking was performed on Rev 0Ba, 0Bb, and 0Bc by Horia R. Radulescu, who has since left the project.

Data Tracking Number SN0410T0510404.002 was not available for viewing in the technical data management system. Access to the file for this Data Tracking Number was granted by Ernest Hardin and provided by Celister Houston on 09/27/2006.

Rev 01 of DIRS 170909 includes administrative changes that have no impact on this calculation.

Attachments	Total Number of Pages
Attachment I – Determination of the Critical Limit	16
Attachment II – Listing of Files Contained in Attachment III	3
Attachment III – Computer Files for Calculation	1 CD-ROM

RECORD OF REVISIONS

9. No.	10. Reason For Revision	11. Total # of Pgs.	12. Last Pg. #	13. Originator (Print/Sign/Date)	14. Checker (Print/Sign/Date)	15. Approved/Accepted (Print/Sign/Date)
00A	Initial issue.	75	II-3	Darby Kimball Dennis Moscalu	Jason Huffer	William E. Hutchins 09/29/2004
0B	To reflect updated DOE SNF and WP design and to evaluate more DOE SNF types. The document status designation has been changed from preliminary to committed because the results are not expected to change in such a manner that will affect support of regulatory submittals. Extensive Revision. All pages are affected.	89	II-3	Charlotta E. Sanders *[signature]* 09/27/2006	Jabo S. Tang *[signature] aadsaid for Jabo Tony 9/29/06*	Abdelhalim A. Alsaed *[signature] aadsaid 9/29/06*
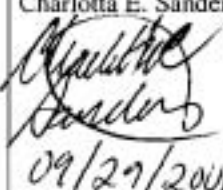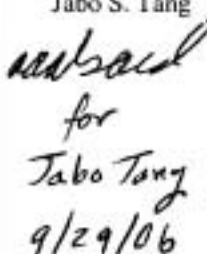
CONTENTS

TABLES

Page

FIGURES

Page

1. PURPOSE

The objective of this calculation is to evaluate the criticality potential for co-disposal waste packages affected by an igneous intrusion disruptive event in the emplacement drifts. The scope of this calculation is limited to U.S. Department of Energy (DOE) Spent Nuclear Fuel (SNF) types in DOE standardized SNF canisters or Multi-Canister Overpack (MCO) Canisters. DOE SNF has been categorized into nine fuel groups for purposes of evaluating criticality safety (DOE 2004, [DIRS 170071], Table A-1). A representative fuel type was chosen for each group as follows [the corresponding DOE fuel group is listed inside brackets]:

- Fast Flux Test Facility (FFTF) [Mixed Oxide fuel]
- Enrico Fermi [Uranium-Zirconium/ Uranium-Molybdenum fuel]
- Fort St. Vrain (FSV) [Uranium/Thorium/Plutonium Carbide fuel]
- Training, Research, and Isotope General Atomics (TRIGA) [Uranium- Zirconium-Hydride fuel]
- Advanced Test Reactor (ATR) [Uranium-Aluminum fuel]
- Three Mile Island (TMI) (debris) [Uranium Oxide (Low Enriched Uranium) fuel]
- N-Reactor [Uranium Metal fuel]
- Shippingport Pressurized Water Reactor (PWR) [Uranium Oxide (High Enriched Uranium) fuel]
- Shippingport Light Water Breeder Reactor (LWBR) [Uranium/Thorium Oxide fuel]

These fuels are slated for codisposal with high level waste (HLW) in either a 5-DHLW/DOE SNF Short Waste Package, a 5-DHLW/DOE SNF Long Waste Package, or a 2-MCO/2-DHLW Waste Package.

In this calculation the effective neutron multiplication factor (k_{eff}) is determined for possible configurations of the waste package during and after an intrusive igneous event. External criticality is not addressed in this calculation (i.e., no material is transported out of the DOE standardized SNF canister) and neither is misloading of waste packages (it is beyond the scope of this calculation).

These calculations are intended to support the *Screening Analysis of Criticality Features, Events, and Processes for License Application* (BSC 2004 [DIRS 168556]). However, there are no limitations on the use of the results of this calculation provided that the boundaries established by the geometrical representations and material compositions and quantities considered in this calculation are not changed.

2. REFERENCES

2.1 DESIGN INPUTS

170284   ASM (American Society for Metals) 1961. "Properties and Selection of Metals."
Volume 1 of *Metals Handbook.* 8th Edition. Lyman, T.; ed. Metals Park, Ohio:
American Society for Metals. TIC: 257281.

133378   ASM International 1987. *Corrosion.* Volume 13 of *ASM Handbook.* Formerly 9th
Edition, Metals Handbook. [Materials Park, Ohio]: ASM International. TIC:
240704.

158115   ASME (American Society of Mechanical Engineers) 2001. *2001 ASME Boiler
and Pressure Vessel Code (includes 2002 addenda).* New York, New York:
American Society of Mechanical Engineers. TIC: 251425.

103515   ASTM G 1-90 (Reapproved 1999). 1999. *Standard Practice for Preparing,
Cleaning, and Evaluating Corrosion Test Specimens.* West Conshohocken,
Pennsylvania: American Society for Testing and Materials. TIC: 238771.

117138   ASTM A 516/A 516M-90 1991. *Standard Specification for Pressure Vessel
Plates, Carbon Steel, for Moderate-and Lower-Temperature Service.* West
Conshohocken, Pennsylvania: American Society for Testing and Materials. TIC:
240032.

104133   ASTM A 276-91a. 1991. *Standard Specification for Stainless and Heat-Resisting
Steel Bars and Shapes.* Philadelphia, Pennsylvania: American Society for Testing
and Materials. TIC: 240022.

168403   ASTM B 932-04. 2004. *Standard Specification for Low-Carbon Nickel-
Chromium-Molybdenum-Gadolinium Alloy Plate, Sheet, and Strip.* West
Conshohocken, Pennsylvania: American Society for Testing and Materials. TIC:
255846.

103515   ASTM G 1-90 (Reapproved 1999). 1999. *Standard Practice for Preparing,
Cleaning, and Evaluating Corrosion Test Specimens.* West Conshohocken,
Pennsylvania: American Society for Testing and Materials. TIC: 238771.

149625   Audi, G. and Wapstra, A.H. 1995. *Atomic Mass Adjustment, Mass List for
Analysis.* [Upton, New York: Brookhaven National Laboratory, National Nuclear
Data Center]. TIC: 242718.

103805   Beyer, W.H., ed. 1987. *CRC Standard Mathematical Tables.* 28th Edition. 3rd Printing 1988. Boca Raton, Florida: CRC Press. TIC: 240507.

103897   Briesmeister, J.F., ed. 1997. *MCNP-A General Monte Carlo N-Particle Transport Code.* LA-12625-M, Version 4B. Los Alamos, New Mexico: Los Alamos National Laboratory. ACC: MOL.19980624.0328.

157195   BSC (Bechtel SAIC Company) 2001. *EQ6 Calculations for Chemical Degradation of Fast Flux Test Facilities (FFTF) Waste Packages: Effects of Updated Design and Rates.* CAL-EDC-MD-000014 REV 00. Las Vegas, Nevada: Bechtel SAIC Company. ACC: MOL.20020102.0191.

156111   BSC (Bechtel SAIC Company) 2001. *Intact and Degraded Mode Criticality Calculations for the Codisposal of Fort Saint Vrain HTGR Spent Nuclear Fuel in a Waste Package.* CAL-EDC-NU-000007 REV 00. Las Vegas, Nevada: Bechtel SAIC Company. ACC: MOL.20011015.0020.

161781   BSC (Bechtel SAIC Company) 2002. *Benchmark and Critical Limit Calculation for DOE SNF.* CAL-EDC-NU-000008 REV 00. Las Vegas, Nevada: Bechtel SAIC Company. ACC: MOL.20020416.0053.

164419   BSC (Bechtel SAIC Company) 2003. *Analysis of Critical Benchmark Experiments and Critical Limit Calculation for DOE SNF.* CAL-DSD-NU-000003 REV 00A. Las Vegas, Nevada: Bechtel SAIC Company. ACC: DOC.20030724.0002.

169107   BSC (Bechtel SAIC Company) 2003. *EQ6 Calculation for Chemical Degradation of Enrico Fermi Codisposal Waste Packages: Effects of Updated Design and Rates.* CAL-EDC-MD-000015 REV 00 [Errata 001]. Las Vegas, Nevada: Bechtel SAIC Company. ACC: MOL.20020102.0190; DOC.20031014.0012.

169980   BSC (Bechtel SAIC Company) 2004. *Characterize Eruptive Processes at Yucca Mountain, Nevada.* ANL-MGR-GS-000002 REV 02. Las Vegas, Nevada: Bechtel SAIC Company. ACC: DOC.20041004.0006; DOC.20050718.0005.

168553   BSC (Bechtel SAIC Company) 2004. *Criticality Model.* CAL-DS0-NU-000003 REV 00A. Las Vegas, Nevada: Bechtel SAIC Company. ACC: DOC.20040913.0008; DOC.20050728.0007.

170028   BSC (Bechtel SAIC Company) 2004. *Dike/Drift Interactions.* MDL-MGR-GS-000005 REV 01. Las Vegas, Nevada: Bechtel SAIC Company. ACC: DOC.20041124.0002; DOC.20050622.0002.

170878   BSC (Bechtel SAIC Company) 2004. *HLW/DOE SNF Codisposal Waste Package Design Report.* 000-00C-DS00-00600-000-00B. Las Vegas, Nevada: Bechtel SAIC Company. ACC: ENG.20040701.0007.

171794   BSC (Bechtel SAIC Company) 2004. *Independent Verification and Validation Report for Legacy Code CLREG Version 1.0.* 10528-SDR-1.0-01. Las Vegas, Nevada: Bechtel SAIC Company. ACC: MOL2004.0317.0145.

168935   BSC (Bechtel SAIC Company) 2004. *Intact and Degraded Mode Criticality Calculations for the Codisposal of TMI-2 Spent Nuclear Fuel in a Waste Package.* CAL-DSD-NU-000004 REV 00A. Las Vegas, Nevada: Bechtel SAIC Company.   ACC: DOC.20040329.0002;   DOC.20050601.0003; DOC.20050801.0001.

171926   BSC (Bechtel SAIC Company) 2004. *Intact and Degraded Mode Criticality Calculations for the Codisposal of ATR Spent Nuclear Fuel in a Waste Package.* CAL-DSD-NU-000007 REV 00A. Las Vegas, Nevada: Bechtel SAIC Company. ACC: DOC.20041018.0001; DOC.20050728.0002.

168556   BSC (Bechtel SAIC Company) 2004. *Screening Analysis of Criticality Features, Events, and Processes for License Application.* ANL-EBS-NU-000008 REV 01. Las Vegas, Nevada: Bechtel SAIC Company. ACC: DOC.20041022.0001.

173284   BSC (Bechtel SAIC Company) 2005. *Canister Handling Facility Criticality Safety Calculations.* 190-00C-CH00-00100-000-00B. Las Vegas, Nevada: Bechtel SAIC Company. ACC: ENG.20050411.0001; ENG.20050803.0003; ENG.20050912.0006; ENG.20050803.0008.

175539   BSC (Bechtel SAIC Company) 2005. *Q-List.* 000-30R-MGR0-00500-000-003. Las Vegas, Nevada: Bechtel SAIC Company. ACC: ENG.20050929.0008.

177193   BSC (Bechtel SAIC Company) 2006. *Dimension and Material Specification Selection for Use in Criticality Analyses.* CAL-DSU-NU-000017 REV 0A. Las Vegas, Nevada: Bechtel SAIC Company. ACC: DOC.20060906.0004.

176911   BSC (Bechtel SAIC Company) 2006. *Geochemistry Model Validation Report: Material Degradation and Release Model.* ANL-EBS-GS-000001 REV 01. Las Vegas, Nevada: Bechtel SAIC Company. ACC: DOC.20060901.0009.

159483   CLReg V. 1.0. 2002. WINDOWS 2000. STN: 10528-1.0-01.

102836   CRWMS M&O 1998. *Software Qualification Report for MCNP Version 4B2, A General Monte Carlo N-Particle Transport Code.* CSCI: 30033 V4B2LV. DI: 30033-2003, Rev. 01. Las Vegas, Nevada: CRWMS M&O. ACC: MOL.19980622.0637.

102140   CRWMS M&O 1999. *DOE SRS HLW Glass Chemical Composition.* BBA000000-01717-0210-00038 REV 00. Las Vegas, Nevada: CRWMS M&O. ACC: MOL.19990215.0397.

104118   CRWMS M&O 1999. *Enrico Fermi Fast Reactor Spent Nuclear Fuel Criticality Calculations: Intact Mode.* BBA000000-01717-0210-00037 REV 00. Las Vegas, Nevada: CRWMS M&O. ACC: MOL.19990125.0079.

103899   CRWMS M&O 1999. *EQ6 Calculations for Chemical Degradation of TRIGA Codisposal Waste Packages.* CAL-EDC-MD-000001 REV 00. Las Vegas, Nevada: CRWMS M&O. ACC: MOL.19991118.0050.

102842   CRWMS M&O 1999. *Fast Flux Test Facility (FFTF) Reactor Fuel Criticality Calculations.* BBA000000-01717-0210-00016 REV 00. Las Vegas, Nevada: CRWMS M&O. ACC: MOL.19990426.0142.

135852   CRWMS M&O 1999. *TRIGA Fuel Phase I and II Criticality Calculation.* CAL-MGR-NU-000001 REV 00. Las Vegas, Nevada: CRWMS M&O. ACC: MOL.19991209.0195; DOC.20050728.0005.

150852   CRWMS M&O 2000. *Enrico Fermi Fast Reactor Spent Nuclear Fuel Criticality Calculations: Degraded Mode.* CAL-EDC-NU-000001 REV 00. Las Vegas, Nevada: CRWMS M&O. ACC: MOL.20000802.0002.

144714   CRWMS M&O 2000. *Intact and Degraded Criticality Calculations for the Codisposal of Shippingport PWR Fuel in a Waste Package.* CAL-EDC-NU-000002 REV 00. Las Vegas, Nevada: CRWMS M&O. ACC: MOL.20000209.0233.

151722   CRWMS M&O 2000. *Intact and Degraded Criticality Calculations for the Codisposal of Shippingport LWBR Spent Nuclear Fuel in a Waste Package.* CAL-EDC-NU-000004 REV 00. Las Vegas, Nevada: CRWMS M&O. ACC: MOL.20000922.0093.

153262   CRWMS M&O 2001. *Intact and Degraded Component Criticality Calculations of N Reactor Spent Nuclear Fuel.* CAL-EDC-NU-000003 REV 00. Las Vegas, Nevada: CRWMS M&O. ACC: MOL.20010223.0060.

160320   D'Agostino, R.B. and Stephens, M.A., eds. 1986. *Goodness-Of-Fit Techniques.* Statistics, Textbooks and Monographs Volume 68. New York, New York: Marcel Dekker. TIC: 253256.

161786   Dean, J.C. and Tayloe, R.W., Jr. 2001. *Guide for Validation of Nuclear Criticality Safety Calculational Methodology.* NUREG/CR-6698. Washington, D.C.: U.S. Nuclear Regulatory Commission. TIC: 254004.

104110   DOE (U.S. Department of Energy) 1999. *Fermi (U-Mo) Fuel Characteristics for Disposal Criticality Analysis.* DOE/SNF/REP-035, Rev. 0. Washington, D.C.: U.S. Department of Energy. TIC: 242461.

104940   DOE (U.S. Department of Energy) 1999. *Shippingport PWR (HEU Oxide) Fuel Characteristics for Disposal Criticality Analysis*. DOE/SNF/REP-040, Rev. 0. Washington, D.C.: U.S. Department of Energy. TIC: 243528.

103891   DOE (U.S. Department of Energy) 1999. *TRIGA (UZrH) Fuel Characteristics for Disposal Criticality Analysis*. DOE/SNF/REP-048, Rev. 0. Washington, D.C.: U.S. Department of Energy. TIC: 244162.

150095   DOE (U.S. Department of Energy) 2000. *N Reactor (U-Metal) Fuel Characteristics for Disposal Criticality Analysis*. DOE/SNF/REP-056, Rev. 0. [Washington, D.C.]: U.S. Department of Energy, Office of Environmental Management. TIC: 247956.

170071   DOE (U.S. Department of Energy) 2004. *Packaging Strategies for Criticality Safety for "Other" DOE Fuels in a Repository*. DOE/SNF/REP-090, Rev. 0. Idaho Falls, Idaho: U.S. Department of Energy, Idaho Operations Office. ACC: MOL.20040708.0386.

148850   MO0003RIB00071.000. Physical and Chemical Characteristics of Alloy 22. Submittal date: 03/13/2000.

162015   DTN: GS000308313211.001. Geochemistry of Repository Block. Submittal date: 03/27/2000.

155989   DTN: MO0109HYMXPROP.001. Matrix Hydrologic Properties Data. Submittal date: 09/17/2001.

172712   SN0410T0510404.002. Thermodynamic Database Input File for EQ3/6 - DATA0.YMP.R4. Submittal date: 11/01/2004.

130835   Inco Alloys International 1988. Product Handbook. Huntington, West Virginia: Inco Alloys International. TIC: 239397.

158820   INEEL (Idaho National Engineering and Environmental Laboratory) 2002. *FFTF (MOX) Fuel Characteristics for Disposal Criticality Analysis*. DOE/SNF/REP-032, Rev. 1. Idaho Falls, Idaho: U.S. Department of Energy, Idaho National Operations Office. TIC: 252933.

154060   MCNP V. 4B2LV. 1998. HP-UX 9.07 & 10.20, WINDOWS 95, SOLARIS 2.6. CSCI: 30033-V4B2LV-.

170909   Moscalu, D.R. 2004. *Analysis of Critical Benchmark Experiments for Configurations External to WP*. 32-5045840-00. Las Vegas, Nevada: Areva. ACC: DOC.20040701.0003.

103886   Natrella, M.G. 1963. *Experimental Statistics*. National Bureau of Standards Handbook 91. Washington, D.C.: U.S. Department of Commerce, National Bureau of Standards. TIC: 245911.

169530   NEA (Nuclear Energy Agency) 2003. *International Handbook of Evaluated Criticality Safety Benchmark Experiments*. 2003 Edition. NEA/NSC/DOC(95)03. [Paris, France]: Nuclear Energy Agency, Organization for Economic Co-Operation and Development. TIC: 256092.

103896   Parrington, J.R., et. al. 1996. *Nuclides and Isotopes, Chart of the Nuclides*. 15th Edition. San Jose, California: General Electric Company and KAPL, Inc. TIC: 233705.

107105   Roberts, W.L.; Campbell, T.J.; and Rapp, G.R., Jr. 1990. *Encyclopedia of Minerals*. 2nd Edition. New York, New York: Van Nostrand Reinhold. TIC: 242976.

154197   Scheaffer, R.L. and McClave, J.T. 1990. *Probability and Statistics for Engineers*. 3rd Edition. Boston, Massachusetts: PWS-Kent. TIC: 249631.

102813   Stout, R.B. and Leider, H.R., eds. 1991. *Preliminary Waste Form Characteristics Report*. Version 1.0. Livermore, California: Lawrence Livermore National Laboratory. ACC: MOL.19940726.0118.

127163   Weast, R.C., ed. 1972. *CRC Handbook of Chemistry and Physics*. 53rd Edition. Cleveland, Ohio: Chemical Rubber Company. TIC: 219220.

165505   YMP (Yucca Mountain Site Characterization Project) 2003. *Disposal Criticality Analysis Methodology Topical Report*. YMP/TR-004Q, Rev. 02. Las Vegas, Nevada: Yucca Mountain Site Characterization Office. ACC: DOC.20031110.0005.

This calculation is based in part on technical information given in Fuel Characteristics reports generated by the National Spent Nuclear Fuel Program (i.e., an outside source) for representative DOE SNF types (i.e., DOE 1999 [DIRS 103891], DOE 1999 [DIRS 104940] and DOE 2000 [DIRS 150095]). Being the waste form custodian, the National Spent Nuclear Fuel Program has safely handled and stored this SNF for many years making them a reliable source of information. These reports are the best and only available input sources that characterize these fuel types. In addition, the following outside input sources were used in this calculation: Inco Alloys International 1988 [DIRS 130835] and Stout and Leider 1991 [DIRS 102813]. The Inco Alloys International 1988 [DIRS 130835] is considered to be a reliable source because the material is used in nuclear applications.   The Stout and Leider 1991 [DIRS 102813] provides a representative input for the glass fill volume and the glass densities (hot and cold). Further, the input data used from these sources have only minor impacts on the results.

2.2   DESIGN CONSTRAINTS

177019   EG-PRO-3DP-G04B-00037, Rev. 3. *Calculations and Analyses.* Las Vegas, Nevada: Bechtel SAIC Company. ACC: ENG.20060522.0002.

176659   IT-PRO-0011, Rev. 0. *Software Management.* Las Vegas, Nevada: Bechtel SAIC Company. ACC: DOC.20060301.0007.

176927   DOE (U.S. Department of Energy) 2006. *Quality Assurance Requirements and Description.* DOE/RW-0333P, Rev. 17. Washington, D.C.: U.S. Department of Energy, Office of Civilian Radioactive Waste Management. ACC: DOC.20060504.0008.

149756   NRC (U.S. Nuclear Regulatory Commission) 2000. *Standard Review Plan for Spent Fuel Dry Storage Facilities.* NUREG-1567. Washington, D.C.: U.S. Nuclear Regulatory Commission. TIC: 247929.

2.3   DESIGN OUTPUTS

This calculation will be used as input for other calculations.

3. ASSUMPTIONS

3.1 ASSUMPTIONS REQUIRING VERIFICATION

3.1.1 HLW Glass Composition

Assumption: It is assumed that the HLW glass in the waste package has the composition of Savannah River Site (SRS) glass.

Rationale: The anticipated composition of SRS glass is available (CRWMS M&O 1999 [DIRS 102140], p. 7). HLW glass in codisposal canisters is expected to be similar to SRS glass. Since the glass primarily acts as a reflector, it is expected that variations in composition will not impact significantly the results of this calculation.

Confirmation: This assumption requires further confirmation (TBV-3022).

Usage: This assumption is used in Sections 6.1 and 6.5.3.

3.1.2 Consistency of Neutron Absorber Material

Assumption: It is assumed that during and after an igneous event, the neutron absorber material alloy (Ni-Gd) will not melt or be displaced due to eutectic interactions with surrounding metals.

Rationale: There is currently no data available to support this assumption so this rationale requires confirmation.

Confirmation: This assumption requires further confirmation (TBV-7724).

Usage: This assumption is used in Section 6.3.2.2.

3.2 ASSUMPTIONS NOT REQUIRING VERIFICATION

3.2.1 HLW Glass Can Move Freely in Package

Assumption: It is assumed that the HLW glass, once melted, is free to move inside the waste package.

Rationale: As discussed in Section 6.3.2.2, the temperature of the magma (or, to be more accurate the temperature of HLW glass and gases reached as a result of thermal contact with magma) is expected to be high enough to overpressurize the interior of the HLW canisters and breach them. In addition, the temperature in the waste package is expected to rise above the melting point of the HLW glass, which is just over 825 °C (see Section 6.3.2.2).   Also, the magma is predicted to have temperatures around 1100 °C (see Section 6.3.1).

Confirmation: This assumption does not require further confirmation by testing, design, or analysis.

Usage: This assumption is used in Section 6.1, Section 6.3.2.2, and Section 6.4.1.

3.2.2 Fuel Composition

Assumption: For non-breeder reactors, it is assumed that all DOE fuel is fresh. Beginning-of-life (BOL) pre-irradiation fuel compositions are used for these calculations. For breeder reactors, driver fuel assemblies are represented as fresh and blanket or breeder assemblies are represented with the most conservative fuel composition (BOL, end of life (EOL), or a composition that bounds BOL and EOL reactivity).

Rationale: This assumption is conservative because in a non-breeder reactor, unirradiated fuel is more neutronically reactive than spent fuel. In a breeder reactor, irradiated fuel may be more reactive than fresh fuel.

Confirmation: This assumption does not require further confirmation by testing

g, design, or analysis.

Usage: This assumption is used in Section 6.

3.2.3   Zinc Represented As Aluminum

Assumption: It is assumed that Al cross-sections may be used instead of Zn cross-sections in the MCNP input.

Rationale: The cross-sections of Zn are not available in the MCNP 4B2LV cross-section libraries. This assumption is conservative for k_{eff} calculations since the thermal neutron capture cross-section and the resonance integral of Zn (Parrington, J.R., et. al. 1996 [DIRS 103896], p. 24) are greater than the thermal neutron capture cross-section and the resonance integral of Al (Parrington, J.R., et. al. 1996 [DIRS 103896], p. 20).

Confirmation: This assumption does not require further confirmation by testing, design, or analysis.

Usage: This assumption is used in Section 6.5.2 and 6.5.3.

3.2.4   Ba-137 Represented As Ba-138

Assumption: It is assumed that Ba-138 cross-sections may be used instead of Ba-137 cross-sections in the MCNP input.

Rationale: The cross-sections of Ba-137 are not available in the MCNP 4B2LV cross-section libraries. This assumption is conservative since the thermal neutron capture cross-section and the resonance integral of Ba-137 (Parrington, J.R., et. al. 1996 [DIRS 103896], p. 34) are greater than the thermal neutron capture cross-section and the resonance integral of Ba-138 (Parrington, J.R., et. al. 1996 [DIRS 103896], p. 34).

Confirmation: This assumption does not require further confirmation by testing, design, or analysis.

Usage: This assumption is used in Section 6.5.3.

3.2.5   Cooled Magma Has Same Porosity as Tuff

Assumption: It is assumed that cooled and fractured magma has the same porosity as tuff.

Rationale: The chemical composition and physical properties of magma and tuff are very similar. According to *Dike/Drift Interactions* (BSC 2004 [DIRS 170028], Assumption 5.4.1 and Assumption 5.4.2), the fracturing and porosity of the cooled intrusive material is expected to be similar to the surrounding tuff.

Confirmation: This assumption does not require further confirmation by testing, design, or analysis.

Usage: This assumption is used in Section 6.3.2.5, Section 6.5.3, and Attachment III.

3.2.6   Waste Package Inner and Outer Barrier Degradation

Assumption: It is assumed that the waste package inner and outer barriers may be represented by their non-degraded volumes and composition for the purposes of this calculation.

Rationale: The waste package inner and outer barriers are deformed and possibly breached during the igneous intrusion, and this is reflected in the calculations. Configurations with all structural material inside completely degraded and the intact DOE standardized SNF canisters under dry and flooded conditions are run. It is expected that the additional moderator added by degrading the waste package barriers will not substantially impact the results. Consequently, the waste package barriers will be represented as deformed where necessary but not degraded.

Confirmation: This assumption does not require further confirmation by testing, design, or analysis.

Usage: This assumption is used in Section 6.4.3.

3.2.7   The Critical Limit

Assumption: It is assumed that the calculated critical limit for Enrico Fermi fuel (0.9673 per Attachment I) also applies to the other DOE SNF considered in this calculation.

Rationale: The *Criticality Model* document (BSC 2004 [DIRS 168553]) calculates the lower-bound tolerance limit of degraded FFTF SNF to be 0.9786 (BSC 2004 [DIRS 168553], p. VII-7), TRIGA SNF to be 0.9796 (BSC 2004 [DIRS 168553], p. IX-17), Fort St. Vrain SNF to be 0.9608 (BSC 2004 [DIRS 168553], p. X-11), Shippingport PWR SNF to be 0.969 (BSC 2004 [DIRS 168553], p. XI-9), Shippingport LWBR to be 0.9748 (BSC 2004 [DIRS 168553], p. IV-11), and N-Reactor SNF to be 0.9748 (BSC 2004 [DIRS 168553], p. VI-9). While the conditions in the *Criticality Model* document are not entirely applicable to the conditions described in this document, most of the calculated tolerance limits are higher than the critical limit calculated for Enrico Fermi SNF in Attachment I. Therefore, it is reasonable to assume that the 0.9673 applies to all DOE SNF for this calculation.

Confirmation: This assumption does not require further confirmation by testing, design, or analysis.

Usage: This assumption is used in Section 6.4.4.

3.2.8   Composition of Pins in Ident-69 Canister (FFTF SNF)

Assumption: It is assumed that densities and the isotopic compositions of Pu and U are the same for the Ident-69 pins and the Type 4.1 driver fuel assembly (DFA).

Rationale: The exact isotopic composition for the fuel pins in the Ident-69 canister is not known. Only the Pu / U ratio is given in source references. Based on the data in (INEEL 2002 [DIRS 158820], Table 1), the isotopic compositions of Pu and U are expected to be approximately the same for all fuels. Type 4.1 fuel has the highest ratio of Pu-239, which is conservative.

Confirmation: This assumption does not require further confirmation by testing, design, or analysis.

Usage: This assumption is used in Section 6.5.1.2 and Attachment III.

3.2.9   Design Specifications of Pins in Ident-69 Canister (FFTF SNF)

Assumption: It is assumed that the total volume of fuel in the source assembly is the same for the Ident-69 pins and the Type 4.1 DFA. It is further assumed that dimensions for the two fuel pins are similar: same length of each component including active fuel length and same cladding thickness.

Rationale: Exact dimensions for the fuel pins in the Ident-69 canister are not known. Only the outer cladding diameter is given in source references. Given the number of fuel pins in each source assembly, an assumption of same volume and active fuel length results in a calculated fuel pellet diameter based on the outer diameter of the Ident-69 fuel rods (Attachment III, file *FFTF.xls*, worksheet "Dimensions"). Other dimensions, such as total pin length and dimensions for structural components, are not expected to significantly impact the reactivity of the fuel.

Confirmation: This assumption does not require further confirmation by testing, design, or analysis.

Usage: This assumption is used in Attachment III.

3.2.10 Impurities in Fermi Fuel

Assumption: It is assumed that the impurities in the Enrico Fermi fuel matrix (B, C, Cr, Fe, N, O, Zr, Cu, and others) may be replaced with molybdenum (Mo).

Rationale: The Enrico Fermi fuel pin material is Uranium/Molybdenum alloy (DOE 1999 [DIRS 104110], p.8). The impurities in the Enrico Fermi fuel matrix only represent trace quantities totaling no greater than 0.5 wt% of the total fuel alloy (DOE 1999 [DIRS 104110], p. 9), which is too low to have any appreciable effect on the calculated eigenvalues. In order to maintain the uranium-to-molybdenum mass ratio, the impurities were represented as molybdenum.

Confirmation: This assumption does not require further confirmation by testing, design, or analysis.

Usage: This assumption is used in Section 6.5.1.3.

3.2.11 Density of GdPO₄ (Fermi SNF)

Assumption: It is assumed that the density of $GdPO_4$ (anhydrous gadolinium phosphate) is 5 g/cm³.

Rationale: No density is reported for $GdPO_4$. However, gadolinium is a rare earth element, and compounds formed by gadolinium will have similar properties to other rare earth compounds. The density of monazite (anhydrous rare earth phosphate containing a mix of rare earth elements) is reported as 5 – 5.3 g/cm³ (Weast, R.C., ed. 1972 [DIRS 127163], p. B-195). The density of $GdPO_4$ is expected to fall into this range. The lower bound of 5 g/cm³ was selected because this results in the smallest mass of Gd in the waste package and is therefore conservative.

Confirmation: This assumption does not require further confirmation by testing, design, or analysis.

Usage: This assumption is used in Section 6.5.1.3 and Attachment III.

3.2.12 Erbium in TRIGA Fuel May Be Neglected

Assumption: It is assumed that there is no erbium in the TRIGA fuel.

Rationale: Some of the TRIGA fuel originally contained erbium as a burnable poison. It is conservative to neglect erbium because its absence results in a higher value for the k_{eff} of the system.

Confirmation: This assumption does not require further confirmation by testing, design, or analysis.

Usage: This assumption is used in Section 6.5.1.7.

3.2.13 Graphite May Be Represented as Commercial Grade Graphite (TRIGA SNF)

Assumption: It is assumed that the density of graphite in the TRIGA SNF is that of graphite commercial grade.

Rationale: The density of the graphite is not expected to substantially impact the results of this calculation. The density of commercial grade graphite is representative of high-density grades of graphite.

Confirmation: This assumption does not require further confirmation by testing, design, or analysis.

Usage: This assumption is used in Section 6.5.1.7.

4. METHODOLOGY

4.1 QUALITY ASSURANCE

This calculation was prepared in accordance with EG-PRO-3DP-G04B-00037 [DIRS 177019], *Calculations and Analyses*, and is subject to the *Quality Assurance Requirements and Description* (DOE 2006 [DIRS 176927]). It concerns engineered barriers (e.g., the waste package) that are included in the *Q-List* (BSC 2005 [DIRS 175539], pp. A-4 and A-7) as items important to safety and waste isolation.

4.2 USE OF SOFTWARE

4.2.1 MCNP

The MCNP code [DIRS 154060] is used to calculate the k_{eff} of the waste package. The software specifications follow:

- Program Name: MCNP [DIRS 154060]
- Version/Revision Number: Version 4B2LV
- Status/Operating System: Qualified/HP-UX B.10.20
- Software Tracking Number: 30033 V4B2LV
- Computer Type: Hewlett Packard (HP) 9000 Series Workstations
- Computer processing unit number: 700887

The input and output files for the various MCNP calculations are included in Attachment III (Attachment II gives the list of the files in Attachment III). The calculation files described in Sections 6 and 7 are such that an independent repetition of the software use may be performed.

The MCNP software used is: (a) appropriate for the application of research and commercial reactor k_{eff} calculations, (b) used only within the range of validation as documented in (Briesmeister, J.F., ed. 1997 [DIRS 103897] and CRWMS M&O 1998 [DIRS 102836]), and (c) obtained from the Software Configuration Management in accordance with procedure IT-PRO-0011 [DIRS 176659], *Software Management*.

4.2.2 CLREG

The CLREG code [DIRS 159483] is used to calculate the lower-bound tolerance limit for the benchmark experiments included in this report and extend the range of applicability for the critical limit (CL). The software specifications follow:

- Program Name: CLREG [DIRS 159483]
- Version/Revision Number: Version 1.0
- Status/Operating System: Qualified/Windows 2000
- Software Tracking Number: 10528-1.0-01
- Computer Type: DELL OPTIPLEX GX240 Personal Computer

The input and output files for the CLREG calculations are included in Attachment III (Attachment II gives the list of the files in Attachment III). The calculation files described in Sections 6 and 7 are such that an independent repetition of the software use may be performed.

The CLREG software used is: (a) appropriate for the calculation of lower-bound tolerance limits, (b) used only within the range of validation as documented in the CLREG documentation (BSC 2004 [DIRS 171794]), (c) obtained from the Software Configuration Management in accordance with procedure IT-PRO-0011 [DIRS 176659], *Software Management*.

4.2.3   Microsoft Excel

The Microsoft Excel software was used for performing arithmetical manipulations in a spreadsheet environment. Manipulations of data to obtain input for MCNP and summaries of results were performed with Excel.

- Title: Excel
- Version/Revision Number: Microsoft® Excel 97 SR-2
- This version is installed on a Dell Optiplex GX260 personal computer with CPU number 503009 running Microsoft Windows 2000, Service Pack 4

The input and output files for the various MCNP calculations are included in Attachment III (Attachment II gives the list of the files on Attachment III).

Microsoft Excel Version 97 SR-2 is an exempt software application in accordance with IT-PRO-0011 [DIRS 176659], Section 1.4.6. The spreadsheets contain sufficient information to allow an independent check to reproduce or verify the results.

4.3   CRITICALITY CALCULATION METHODOLOGY

The calculation method consists of using MCNP Version 4B2LV [DIRS 154060] to determine the effective neutron multiplication factor of the waste package. The calculations are performed using the continuous-energy cross-section libraries, which are part of the qualified code system.

5. LIST OF ATTACHMENTS

ATTACHMENT I   Determination of the Critical Limit (16 pages).

ATTACHMENT II   Listing of Files Contained in Attachment III (3 pages).

ATTACHMENT III   One compact disc (CD) containing MCNP input and output files, CLREG files, and the Excel spreadsheets used in the calculation process.

6. CALCULATION

This section describes the calculations performed to evaluate the k_{eff} of waste packages containing high-level waste material and DOE SNF during and after an igneous intrusion event. Section 6.1 describes the waste packages and their contents. Section 6.2 describes the individual DOE SNF types and their arrangement in the DOE SNF disposable canisters. Section 6.3 describes the igneous intrusion event and its impact on the waste package. Section 6.4 describes the specific calculations made for each waste package. Section 6.5 gives the composition of the materials used in this calculation. The basic formulas used in this calculation are listed in Section 6.6. The results of the calculations are presented in Section 7. The MCNP input and output files developed for this calculation, as well as the spreadsheets used to prepare the MCNP input files, are presented in Attachment III.

This calculation is based in part on technical information given in Fuel Characteristics reports generated by the National Spent Nuclear Fuel Program for representative DOE SNF types, which has been compiled and doumented in detail in the *Dimension and Material Specification Selection for Use in Criticality Analyses* document (BSC 2006 [DIRS 177193]). It should also be mentioned that all DOE fuel is assumed to be fresh for non-breeder reactors and that for breeders reactors the most conservative fuel composition is used (Assumption 3.2.2).

The International System of units (SI) values used in this document are cited as given in the source documents where precise SI values were available. In rare cases where SI values were not available or the provided SI values were imprecise, English system values have been converted to SI units. Such conversions are listed with the SI value first, followed by the English value from the source document in parentheses. The differences that might exist between the dimensions listed here and the dimensions cited in the source documents have no effect on the calculation and should not be interpreted as an indication of accuracy. The number of digits in the values cited herein may be the result of a conversion or may reflect the input from another source; consequently, the number of digits should not be interpreted as an indication of accuracy.

6.1 WASTE PACKAGE DESCRIPTIONS

To simplify the MCNP calculation, the components of the waste packages such as DOE SNF disposable canisters, tubes, end fittings, and fuel pins are represented as right prisms or right circular cylinders. In most cases, this is accomplished by conserving volume but changing geometry, i.e., replacing a region with an irregular shape of structural material with two cylindrical regions (one of structure and one of void) having the proper volumes. In a few other cases structural material was removed or fuel material was added to achieve a right prism or right circular cylinder (as in the case of dished fuel pellets represented as right circular cylinders). Geometry of structural material does not significantly affect reactivity as long as the approximate thickness is conserved. Removing structural material is conservative because the structural material is composed mainly of neutron absorbers, and hence its absence provides a higher value for the k_{eff} of the system. Addition of fuel material is conservative because it adds fissile material and increases the reactivity of the system.

It should also be mentioned that some components of the waste packages (i.e., the canisters

holding the HLW glass, the waste package interior structure, baskets in the DOE SNF disposable canisters, and other stainless steel components) are neglected. This is conservative since these components are composed of neutron absorbing materials.

Description of the 5-DHLW/DOE SNF Short Waste Package, 5-DHLW/DOE SNF Long Waste Package, 2-MCO/2-DHLW Short Waste Package, High-Level Waste Pour Canisters, DOE Standardized SNF Canisters, and Multi-Canister Overpack (MCO) Canisters are presented in the *Dimension and Material Specification Selection for Use in Criticality Analyses* document (BSC 2006 [DIRS 177193], Section 6.2).

The HLW glass canister for the 5-DHLW/ DOE SNF short waste package is a stainless steel Type 304L canister with an outer diameter of 61 cm (24 in.) and a nominal length of 3.00 m (118 in.), (BSC 2004 [DIRS 170878], Table 9). The HLW glass canister for the 5-DHLW/ DOE SNF long waste package and the 2-MCO/2-DHLW waste package is a stainless steel Type 304L canister with an outer diameter of 61 cm (24 in.) and a nominal length of 4.57 m (180 in.), (BSC 2004 [DIRS 170878], Table 9). The expected glass fill volume is 85% when poured and approximately 80% when cooled (Stout, R.B. and Leider, H.R., eds. 1991 [DIRS 102813], p. 2.2.1.1-4).

For these calculations, the HLW pour canister has been neglected. The glass is represented as free to move inside the waste package (Assumption 3.2.1). The amount of glass available in one short HLW canister is considered to be 0.59 m^3 at 25 °C (Stout, R.B. and Leider, H.R., eds. 1991 [DIRS 102813], p. 2.2.1.1-4). The amount of glass available in one long HLW canister is considered to be 0.90 m^3 at 25 °C (scaled from the short HLW canister according to canister length).

The borosilicate glass intended for the canisters has yet to be specified in terms of composition, physical properties, etc. However, the resulting glass composition should be similar to that produced at Savannah River Site. The glass is therefore represented as SRS glass (Assumption 3.1.1).

6.2 DOE SNF DESCRIPTIONS

Within the DOE standardized SNF canister or MCO, each fuel has a different arrangement. This calculation identifies nine representative fuels in keeping with the groupings identified by the National Spent Nuclear Fuel Program for criticality calculations (DOE 2004 [DIRS 170071], Table A-1). For each fuel group, a "representative" fuel type within that group is used to establish limits, e.g., burnup, fissile content, weights, and dimensions. The groups and the fuel types chosen to represent each group are shown in Table 6.2-1.

Table 6.2-1. Fuel Groups and Representative Fuel Types

Group Number	Fuel Group	Representative Fuel Type
1	Uranium Metal	N-Reactor
2	Mixed Oxide (UO_2 and PuO_2)	Fast Flux Test Facility
3	U-Mo / U-Zr	Enrico Fermi Fast Reactor
4	Highly Enriched Uranium Oxide (UO_2)	Shippingport PWR
5	Uranium / Thorium Oxide	Shippingport LWBR
6	Graphite / Carbide	Fort St. Vrain
7	U-Zr-H_x	TRIGA
8	Aluminum-based	Advanced Test Reactor
9	Low Enriched Uranium Oxide (UO_2)	Three Mile Island (debris)

Criticality calculations for most of these fuels have been previously performed. Table 6.2-2 summarizes the results available for intact waste packages when loaded in a manner similar to the design loading. It is important to note that the values presented here do not represent the most reactive configurations for each fuel. Instead, the previously evaluated configurations that are most similar to the design configuration have been selected. Due to the limited range of configurations considered in each previous calculation, the dry and flooded cases presented in Table 6.2-2 for each fuel may not be the same geometric configuration. In addition, the Table 6.2-2 results are often not the same configuration as the cases evaluated in this calculation, and are not to be compared to the results presented in Section 7. The values in Table 6.2-2 are used only to gain a general idea of the reactivity of each type of DOE standardized SNF canister or MCO canister.

All fuels listed in this table are modeled with one DOE standardized SNF canister per waste package with the exception of N-Reactor fuel, which has 2 MCO canisters per waste package.

Table 6.2-2. Previous Criticality Results for Waste Packages of Representative Fuels

Group Number	Representative Fuel	Flooded [a] Case ID	Flooded k_{eff} +2σ	Dry [a] Case ID	Dry k_{eff} + 2σ	Reference
1	N-Reactor	1ev02g1	0.8886	Not available		CRWMS M&O 2001 [DIRS 153262], p. 61
2	Fast Flux Test Facility [b]	combo1+5b _ss_10a_w _1a_gd_.5_ 1.6	0.9188 [e]	caseoutid_. 0	0.7536 [c,e]	CRWMS M&O 1999 [DIRS 102842], pp. 32 and 34
3	Enrico Fermi Fast Reactor	slwfgd	0.8706 [c,e]	ilwfg0	0.4119 [e]	CRWMS M&O 1999 [DIRS 104118], pp. 33 and 31
4	Shippingport PWR	sce1.wet1	0.8437 [d]	sce1.dry2	0.1660	CRWMS M&O 2000 [DIRS 144714], p. 32
5	Shippingport LWBR	cod1+al1_. 1	0.8537	cod1_.2	0.4374 [c,e]	CRWMS M&O 2000 [DIRS 151722], p. 39
6	Fort St. Vrain	cs1aL	0.9144	cs1drya	0.7796 [c]	BSC 2001 [DIRS 156111], pp. 40 and 41
7	TRIGA	intact	0.7890 [d,e]	indry	0.6253 [e]	CRWMS M&O 1999 [DIRS 135852], pp. 36 and 37
8	Advanced Test Reactor	atr_int_1a-s	0.6259 [c]	atr_int_1a-s-dry	0.0698	BSC 2004 [DIRS 171926], p. 30
9	Three Mile Island (debris)	wp1a_l_tt	0.9461 [e]	wp1a_l_tt-w	0.3079 [e]	BSC 2004 [DIRS 168935], pp. 46 and 49

NOTES: [a] Except where noted otherwise, flooded cases are cases with completely dry DOE SNF disposable canister(s) and a flooded waste package. Dry cases are cases with dry DOE SNF disposable canister(s) and a dry waste package.
[b] The loading of this DOE standardized SNF canister changed after the intact criticality calculations were performed. Criticality calculations for the new intact configuration are not available.
[c] These cases represent partial flooding of the DOE SNF disposable canister(s); some volumes inside the DOE SNF disposable canister(s) are dry.
[d] These cases represent total flooding of the waste package; both the DOE SNF disposable canister(s) and waste package are flooded.
[e] These cases do not include added neutron absorber, which has been determined necessary through calculations.

The k_{eff} results in Table 6.2-2 indicate that the most reactive representative fuels for flooded conditions are TMI, FFTF, and FSV. For dry conditions, the most reactive representative fuels are FSV, FFTF, and TRIGA. While all nine representative fuels were considered for Calculation Set A (Damage scenarios - see Section 6.4.1) and Calculation Set B (Drift scenarios - see Section 6.4.2), only FFTF, Enrico Fermi, TRIGA, and TMI SNF were considered for Calculation Set C (Degradation Scenarios – see Section 6.4.3). This selection of DOE SNF is based in part on Table 6.2-2, which shows that these DOE fuel types are some of the more reactive fuel types. The number of calculations for the degraded scenarios was also reduced because the bathtub configuration is not expected to reasonably occur (see Section 6.3.2.7) and is only included in this calculation for conservatism.

6.2.1   Uranium Metal SNF (N-Reactor)

The MCNP input model representing N-Reactor fuel in a canister utilized the existing MCNP input file *nr1A-s0* from *Canister Handling Facility Criticality Safety Calculations* (BSC 2005 [DIRS 173284]) as a starting point for the present calculations. The various waste package configurations and surrounding canister HLW glass configurations (see Section 6.4) were added to the previously existing MCNP input files.

The Mark 1A fuel was considered in this calculation and is shown inside the canister in Figure 6.2-1. The geometry of the fuel and canister is documented in the *Canister Handling Facility Criticality Safety Calculations* (BSC 2005 [DIRS 173284], Section 5.1.4.1) and the material specifications are presented in Section 6.5.1.1.
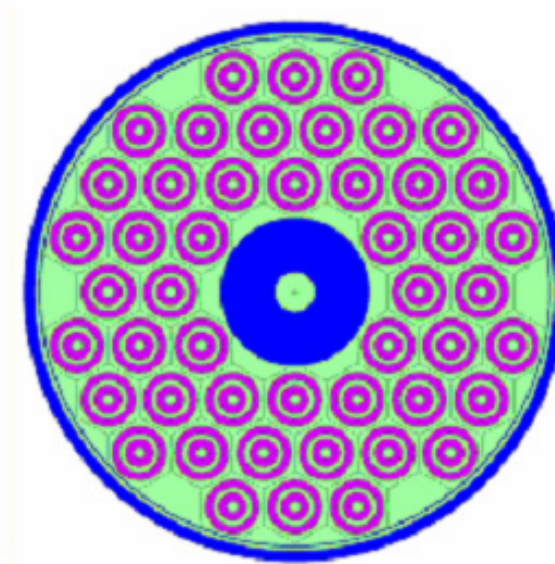
Figure 6.2-1   Top View of DOE Canister Containing Mark 1A Fuel

6.2.2   Mixed Oxide Fuel (Fast Flux Test Facility)

The FFTF fuel is intended for disposal in the long DOE standardized SNF canister and the 5-DHLW/DOE SNF long waste package. The description of the FFTF fuel and canister is documented in the *Dimension and Material Specification Selection for Use in Criticality Analyses* document (BSC 2006 [DIRS 177193], Section 6.3.2.9) and the material specifications are presented in Section 6.5.1.2. Figure 6.2-2 shows the radial cross-sectional view of a DOE canister containing FFTF fuel.
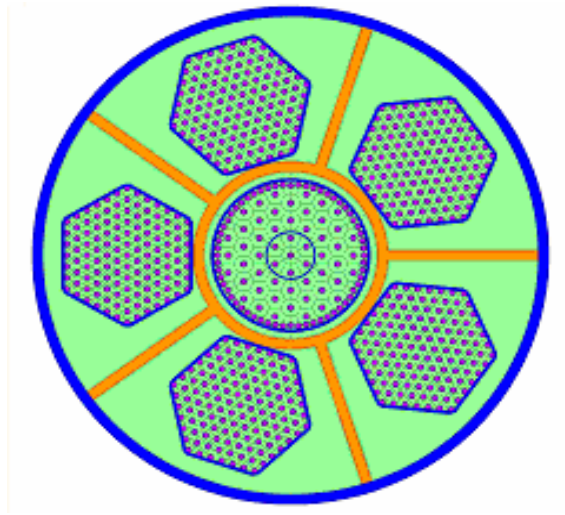
Figure 6.2-2   Top View of DOE Canister Containing FFTF Fuel.

6.2.3   U-Mo / U-Zr SNF (Enrico Fermi Fast Reactor)

The Enrico Fermi fuel is intended for disposal in the short DOE standardized SNF canister and the 5-DHLW/DOE SNF short waste package. The description of the Enrico Fermi fuel and canister interior is from the *Dimension and Material Specification Selection for Use in Criticality Analyses* document (BSC 2006 [DIRS 177193], Section 6.3.2.3) and the material specifications are presented in Section 6.5.1.3. Figure 6.2-3 shows the radial cross-sectional view of a DOE canister containing Enrico Fermi fuel.
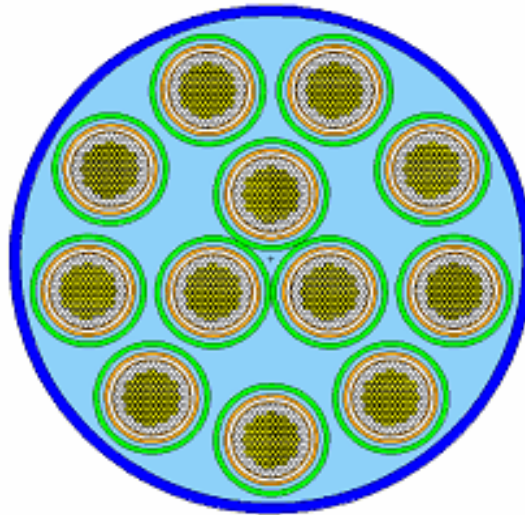
Figure 6.2-3   Top View of DOE Canister Containing Enrico Fermi Fuel.

6.2.4   Highly-Enriched Uranium Oxide SNF (Shippingport PWR)

The MCNP input model representing Shippingport PWR fuel in a canister utilized the existing MCNP input file *sh-ps0* from *Canister Handling Facility Criticality Safety Calculations* (BSC 2005 [DIRS 173284]) as a starting point for the present calculations. The various waste package configurations and surrounding canister HLW glass configurations (see Section 6.4) were added to the previously existing MCNP input files.

Figure 6.2-4 illustrates the radial view of the DOE canister containing Shippingport PWR fuel. The description of the Shippingport PWR fuel and canister is documented in the *Dimension and Material Specification Selection for Use in Criticality Analyses* document (BSC 2006 [DIRS 177193], Section 6.3.2.6) and the material specifications are described in Section 6.5.1.4.
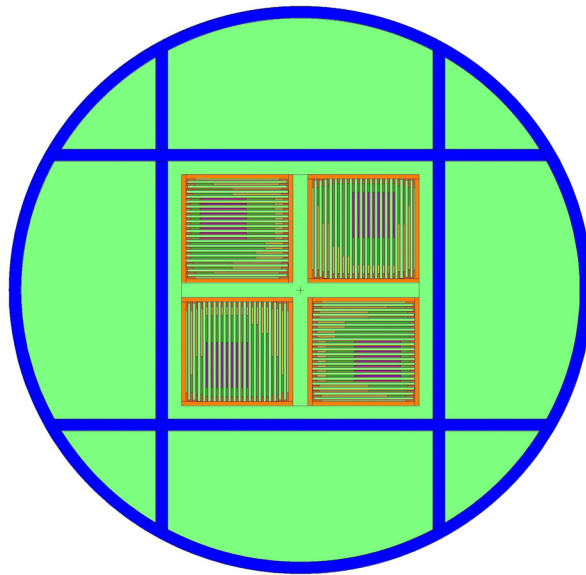
Figure 6.2-4   Top View of DOE Canister Containing Shippingport PWR Fuel.

6.2.5   Uranium / Thorium Oxide SNF (Shippingport LWBR)

 The MCNP input model representing Shippingport LWBR fuel in a canister utilized the existing MCNP input file *sh-ls0* from *Canister Handling Facility Criticality Safety Calculations* (BSC 2005 [DIRS 173284]) as a starting point for the present calculations. The various waste package configurations and surrounding canister HLW glass configurations (see Section 6.4) were added to the previously existing MCNP input files.

Figure 6.2-5 illustrates the radial view of the DOE canister containing Shippingport LWBR fuel. The description of the Shippingport LWBR fuel and canister is documented in the *Dimension and Material Specification Selection for Use in Criticality Analyses* document (BSC 2006 [DIRS 177193], Section 6.3.2.5) and the material specifications are described in Section 6.5.1.5.
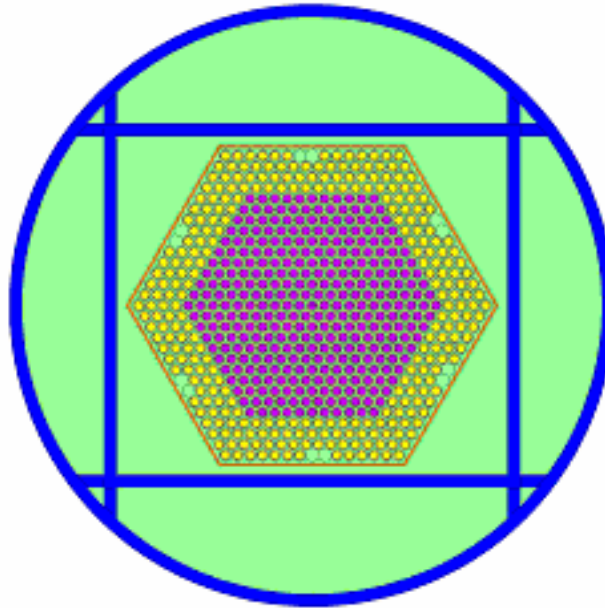
Figure 6.2-5   Top View of DOE Canister Containing Shippingport LWBR Fuel.

6.2.6   Graphite / Carbide SNF (Fort St. Vrain)

The Fort St. Vrain fuel is intended for disposal in the long DOE standardized SNF canister and the 5-DHLW/DOE SNF long waste package. The description of the Fort St. Vrain fuel and canister interior is from the *Dimension and Material Specification Selection for Use in Criticality Analyses* document (BSC 2006 [DIRS 177193], Section 6.3.2.2) and the material specifications are presented in Section 6.5.1.6. Figure 6.2-6 illustrates the radial cross-sectional view of a DOE canister containing Fort St. Vrain fuel.
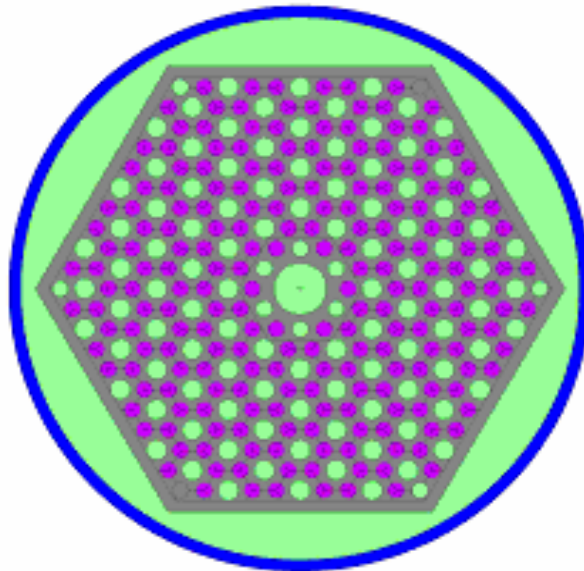
Figure 6.2-6   Top View of DOE Canister Containing Fort St. Vrain Fuel.

6.2.7   U-Zr-H$_x$ SNF (TRIGA Reactor)

The TRIGA fuel is intended for disposal in the short DOE standardized SNF canister and the 5-DHLW/DOE SNF short waste package. The description of the TRIGA fuel and canister interior is from the *Dimension and Material Specification Selection for Use in Criticality Analyses* document (BSC 2006 [DIRS 177193], Section 6.3.2.1) and the material specifications are presented in Section 6.5.1.7. Figure 6.2-7 illustrates the radial cross-sectional view of a DOE canister containing TRIGA fuel.
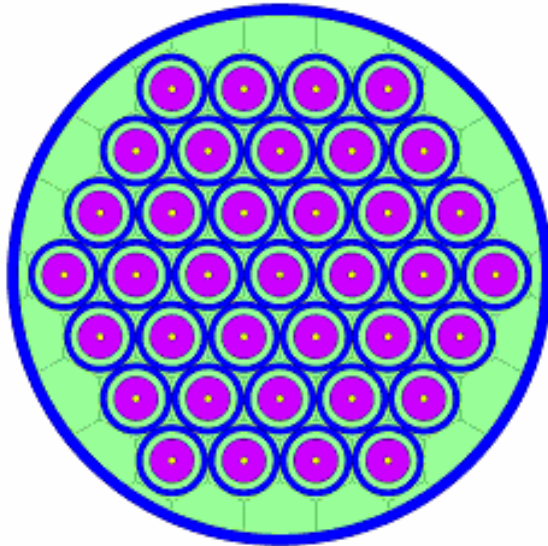
Figure 6.2-7   Top View of DOE Canister Containing TRIGA Fuel.

6.2.8   Aluminum-Based SNF (Advanced Test Reactor)

The Advanced Test Reactor fuel is intended for disposal in the short DOE standardized SNF canister and the 5-DHLW/DOE SNF short waste package. The description of the ATR fuel and canister is documented in the *Dimension and Material Specification Selection for Use in Criticality Analyses* document (BSC 2006 [DIRS 177193], Section 6.3.2.4) and the material specifications are presented in Section 6.5.1.8. Figure 6.2-8 illustrates the radial cross-sectional view of a DOE canister containing ATR fuel.
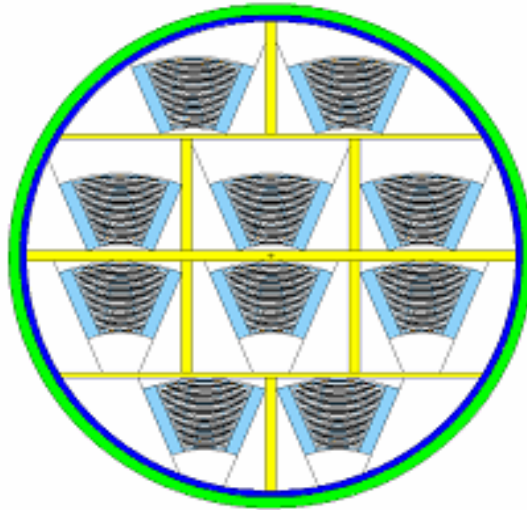
Figure 6.2-8   Top View of DOE Canister Containing ATR Fuel.

6.2.9   Low-Enriched Uranium Oxide (Three Mile Island)

The TMI fuel debris, originated from TMI Unit 2, is intended for disposal in the long DOE standardized SNF canister and the 5-DHLW/DOE SNF long waste package. The description of the TMI fuel and canister is documented in the *Dimension and Material Specification Selection for Use in Criticality Analyses* document (BSC 2006 [DIRS 177193], Section 6.3.2.7) and the material specifications are presented in Section 6.5.1.9. Figure 6.2-9 illustrates the radial cross-sectional view of a DOE canister containing TMI fuel.
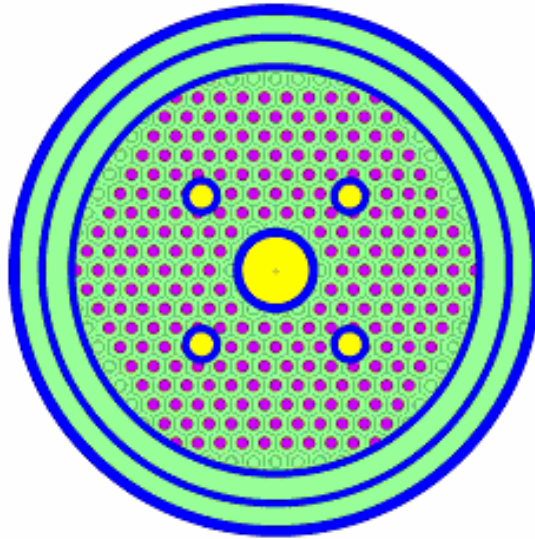
Figure 6.2-9   Top View of DOE Canister Containing TMI Fuel.

6.3   IGNEOUS INTRUSION DESCRIPTION

6.3.1   Description of Initiating Event

The igneous intrusion scenario features an igneous basaltic dike (magma filled crack) that intersects one or more repository drifts, followed by flow of magma into the drifts (BSC 2004 [DIRS 170028], Section 1.1). It is possible during igneous intrusion events that magma or pyroclastic debris will occupy the entire emplacement drift volume around a waste package (BSC 2004 [DIRS 170028], Figures 6-51 & 6-52). The intruding magma or pyroclastic flow is predicted to have a maximum temperature in excess of 1100 °C (BSC 2004 [DIRS 170028], Section 6.4.8.1).

6.3.2   Possible Subsequent Events

6.3.2.1 Waste Package Destroyed

It is expected for igneous intrusion events that the drip shields are damaged (BSC 2004 [DIRS 170028], Section 6.4.8.1). This calculation conservatively does not take credit for the drip shields or invert in predicting damage to the waste packages. For magmatic intrusions, the waste package pallet would also be expected to fail because the structural integrity of the pallet is compromised. This would result in the slumping and flattening of the waste package onto the invert surface.

It is not likely that the entire waste package is destroyed and all of its contents dispersed (BSC 2004 [DIRS 170028], Section 6.4.8.1). Therefore, this calculation does not consider the scenario

of complete dispersal of the waste package contents. However, the possibility does exist for portions of the waste package barrier to be impacted by the igneous intrusion. Consequently, this criticality analysis conservatively includes cases corresponding to destruction and removal of the waste package barrier (though the contents remain in place).

6.3.2.2 Waste Package Slumps and Breaches

As stated in *Dike/Drift Interactions* (BSC 2004 [DIRS 170028], Section 6.4.8.1), at the high temperatures of an igneous intrusion the tensile strength of the waste package and internal components are decreased significantly. The materials are expected to creep readily and fail by mechanical rupture under very small loads, such as the static load from the intrusive material-filled drifts. In addition, the pressure due to gas expansion inside the waste packages and internal canisters may reach the tensile strength of the package materials (BSC 2004 [DIRS 170028], Section 6.4.8.1). Because the magma is expected to maintain elevated temperatures (above 700 °C for 50 to 100 days (BSC 2004 [DIRS 170028], Section 6.4.8)), the waste package internals would similarly have creep failure to the internal components.

This slumping of the waste package and internals would result in the elimination of most of the waste package's internal void spaces. However, there is no expectation that most of the components or materials will relocate from their locations relative to each other. This is reasonable given that intrusion temperatures do not exceed the melting temperatures of the majority of the waste package or waste form component materials. In addition, it is assumed that the neutron absorber material alloy (Ni-Gd) will not melt or be displaced due to eutectic interactions with surrounding metals (Assumption 3.1.2).

The exception to this is the vitrified HLW, which has a melting point of just over 825 °C (Stout, R.B. and Leider, H.R., eds. 1991 [DIRS 102813], p. 2.2.1.1-4). The HLW glass is expected to melt and may drain out of the breached HLW canisters. This calculation assumes that HLW glass is free to move about the interior of the waste package (Assumption 3.2.1).

Three slumping scenarios are considered in this calculation: intact (no slumping or breaching), partial (slumped and breached but all glass is present), and complete (slumped and breached with most of the glass drained out of the waste package).

6.3.2.3 Magma Intrusion into Waste Package

Because the waste package is likely to breach, the possibility for magma to enter the waste package exists. When a waste package breaches the amount of magma that enters the waste package is dependent on the surrounding stresses and on the temperature of the waste package. If the waste package has not yet heated to a temperature near that of the magma, then the initial magma entering the package may cool rapidly near the breach and block additional magma from entering the package. Since the response of the magma in the waste package is uncertain, this calculation considers cases corresponding to magma intrusion and non-intrusion.

6.3.2.4 Magma Cools

Because the drift is expected to remain at elevated temperatures (above 700 °C) for over 50 days (BSC 2004 [DIRS 170028], Section 6.4.8), pre- and post-cooling scenarios must be considered. Since the mineral formation in the magma during cooling cannot be accurately predicted, this calculation treats the magma as a homogenous mixture with the higher density of cooled magma.

6.3.2.5 Magma Fractures After Cooling

As the magma cools, the resulting density change may result in cracking or fracturing. The fracturing and porosity of the cooled intrusive material is assumed to be similar to the surrounding tuff (Assumption 3.2.5). The case of fractured magma before seepage returns is considered to be equivalent or bounded by the case of non-fractured magma from a criticality standpoint because the latter case provides more neutron reflection.

6.3.2.6 Seepage Returns

As the magma cools, natural seepage will return to the drift. If the magma has not fractured during cooling, it may form a natural barrier between seepage and the waste package. Fractures might provide a pathway for seepage to reach the waste package. Depending on the size and nature of the fractures, this seepage rate could be higher or lower than the seepage rate predicted for an undisturbed drift for lithophysae zones. This calculation considers the cases of no seepage (dry magma) and seepage (voids in magma and tuff filled with water).

6.3.2.7 Bathtub Configuration Forms

As in non-igneous scenarios, water may find its way into the waste package. Since the engineered barriers (waste package, DOE standardized SNF canister, fuel cladding) are expected to be damaged during the igneous intrusion, they can no longer be relied upon as a barrier against water. These breaches are expected to impact the bottom of the waste package as well, and thus a bathtub configuration (a pool or closed-bottom container) is not expected to form. However, this calculation conservatively includes some cases that feature full flooding of the waste package.

A more likely scenario is a flow-through configuration, where water is free to pass into and out of the waste package. For this calculation, a dry condition was also modeled, since this has the minimum hydrogen content, and thus provides a complete range of moderator conditions.

6.3.2.8 Fissile Material Transported From Waste Package

In a flow-through configuration or in a fully flooded bathtub configuration, material may be flushed out of the waste package. Depending on chemistry, some materials may be selectively transported out of the waste package. This calculation does not consider the scenario of fissile material transport. The possibility of near-field or far-field criticality due to fissile material collecting outside the waste package is not addressed by this calculation.

6.3.2.9 Degradation of Waste Form

Due to the presence of water, the waste form will degrade. Several degradation configurations are identified in the *Disposal Criticality Analysis Methodology Topical Report* (YMP 2003 [DIRS 165505], Figures 3-2a, 3-2b, 3-3a, and 3-3b). These configurations address both bathtub and flow-through conditions, as well as the order of degradation for the internal waste package components.

For the current calculation, it was reasoned that degraded configurations that retained fissile material in a concentrated form would be more reactive. In addition, degradation products that act as moderating material will increase the reactivity of the system. For this reason, the degradation scenarios addressed in this calculation feature degradation products with high hydrogen ratios that have formed in place in the DOE standardized SNF canister. It is expected that this is a bounding set of degradation scenarios for igneous events. However, the degraded criticality analyses for each SNF type (CRWMS M&O 2000 [DIRS 150852] and CRWMS M&O 1999 [DIRS 135852]) should be the primary source for conclusions regarding degraded configurations. Those analyses feature conservative reflection and moderation conditions and are expected to bound any possible igneous scenarios.

6.3.3   Scenarios Selected for Consideration

Based on the previous discussion, the following scenarios presented in Table 6.3-1 will be considered for each SNF type.

Table 6.3-1. Igneous Intrusion Scenarios Selected For Consideration

Waste Package Destroyed	Waste Package Slumps and Breaches	Magma Intrusion into Waste Package	Magma Cooled	Magma Fractures After Cooling	Seepage Returns	Bathtub Config Formed	Waste Form Degraded Config
N	Intact	N	N	---	---	---	---
N	Intact	N	Y	N	---	---	---
N	Intact	N	Y	Y	N [a]	---	---
N	Intact	N	Y	Y	Y	N	various
N	Partial	N	N	---	---	---	---
N	Partial	N	Y	N	---	---	---
N	Partial	N	Y	Y	N [a]	---	---
N	Partial	N	Y	Y	Y	N	various
N	Partial	N	Y	Y	Y	Y	various
N	Partial	Y	N	---	---	---	---
N	Partial	Y	Y	N	---	---	---
N	Partial	Y	Y	Y	N [a]	---	---
N	Partial	Y	Y	Y	Y	N	various
N	Partial	Y	Y	Y	Y	Y	various
N	Complete	N	N	---	---	---	---
N	Complete	N	Y	N	---	---	---
N	Complete	N	Y	Y	N [a]	---	---
N	Complete	N	Y	Y	Y	N	various
N	Complete	N	Y	Y	Y	Y	various
N	Complete	Y	N	---	---	---	---
N	Complete	Y	Y	N	---	---	---
N	Complete	Y	Y	Y	N [a]	---	---
N	Complete	Y	Y	Y	Y	N	various
N	Complete	Y	Y	Y	Y	Y	various
Y	Partial	N	N	---	---	---	---
Y	Partial	N	Y	N	---	---	---
Y	Partial	N	Y	Y	N [a]	---	---
Y	Partial	N	Y	Y	Y	N	various
Y	Partial	N	Y	Y	Y	Y	various
Y	Partial	Y [b]					
Y	Complete	N	N	---	---	---	---
Y	Complete	N	Y	N	---	---	---
Y	Complete	N	Y	Y	N [a]	---	---
Y	Complete	N	Y	Y	Y	N	various
Y	Complete	N	Y	Y	Y	Y	various
Y	Complete	Y	N	---	---	---	---
Y	Complete	Y	Y	N	---	---	---
Y	Complete	Y	Y	Y	N [a]	---	---
Y	Complete	Y	Y	Y	Y	N	various
Y	Complete	Y	Y	Y	Y	Y	various

NOTES: [a] Cases with magma fracture are neutronically bounded by cases with no magma fracture. The cases with magma fracture and no seepage will not be considered individually (Section 6.3.2.5).
[b] When both waste package and glass are absent, partial slumping is identical to complete slumping (Section 6.4.1).

6.4   CRITICALITY CALCULATIONS

Due to the large number of scenarios in Table 6.3-1, these scenarios are organized into three sets (Set A, Set B and Set C). The DOE SNF is then considered in these three sets of conditions. A detailed description of the three sets is provided below.

6.4.1   Damage Scenarios (Calculation Set A)

First, the damage scenarios are considered (Calculation Set A). The events included in the damage scenario subset are:

- Waste package destroyed
- Waste package slumps and breaches
- Magma intrusion into waste package / HLW glass carried away

The first event (destruction of waste packages) has two possible states: the waste package is not destroyed and is therefore present, or the waste package is destroyed and the inner and outer barriers are replaced with magma. Note that the presence of the waste package is independent of the presence of HLW glass (treated in the third event).

The second event is considered with three different slumping configurations: intact, partial slump, and complete slump. In all three cases the HLW glass is melted and capable of migrating from its original location (Assumption 3.2.1). In the intact configuration the waste package has not breached or deformed. The glass has been represented as a cylinder around the DOE standardized SNF canister. In the partial slump case, the waste package has deformed and breached under the weight of the surrounding magma, but none of the glass has been forced out of the waste package. The voids in the waste package are gone, and the waste package has slumped into a semi-cylindrical geometry so the DOE standardized SNF canister is resting at the bottom of the waste package near the tuff. In the complete slump case, the waste package has deformed and breached, and the weight of the magma has forced most of the HLW glass out of the package. Diagrams of each of these configurations may be found in Table 6.4-1.

The third event is treated by replacing HLW glass with magma. In cases where the waste package is present, this represents magma intrusion into the waste package. In cases where the waste package is not present, this represents the HLW glass being carried away by magma. Note that the partial and complete slump configurations are identical when both the waste package and the HLW glass are not present.

These three events are examined with eight damage scenarios, detailed below. All cases in this subset were run with heated magma and no return of seepage. All cases in this subset were of flow-through configuration 0, representing dry and non-degraded fuel (as described in Section 6.4.3).

The results from Calculation Set A are examined to find the most reactive damage scenario in the set. This damage scenario is used in the drift scenario subset (Section 6.4.2). In addition, the results are examined to determine the change in reactivity between the most reactive and least reactive damage scenarios. This difference is labeled Δk_{damage}.

Table 6.4-1. Damage Scenarios

Waste Package Destroyed	Waste Package Slumps and Breaches	Magma Intrusion into Waste Package	Configuration Designation	Diagram
N	Intact	N	wig	
N	Partial	N	wpg	
N	Partial	Y	wpx	
N	Complete	N	wcg	
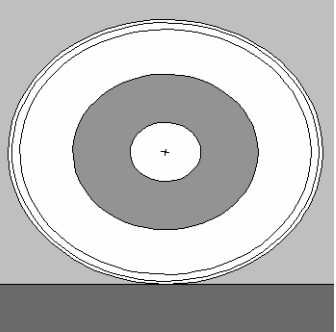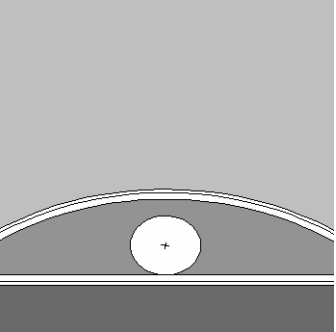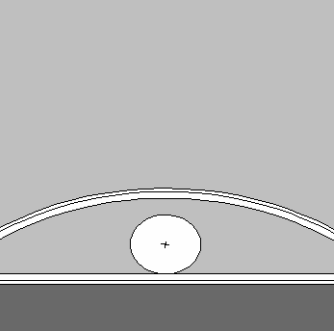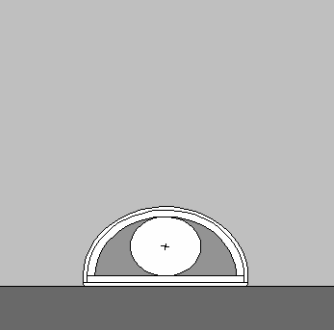
Table 6.4-1 continued. Damage Scenarios

Waste Package Destroyed	Waste Package Slumps and Breaches	Magma Intrusion into Waste Package	Configuration Designation	Diagram
N	Complete	Y	wcx	
Y	Partial	N	xpg	
Y	Partial	Y	N/A [a]	
Y	Complete	N	xcg	
Y	Complete	Y	xcx	
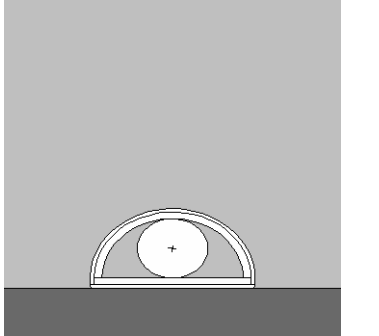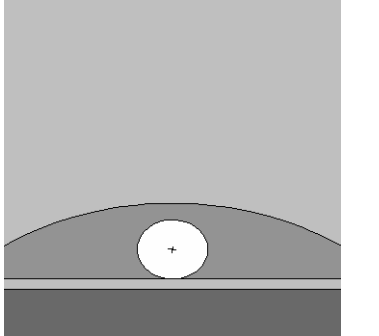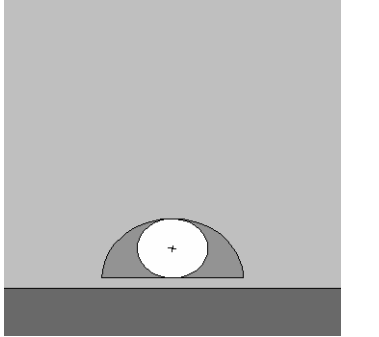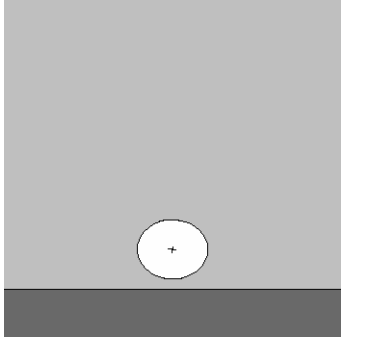
NOTES: [a] The partially slumped case with no waste package and no glass present is geometrically identical to the slumped case with no waste package and no glass. The partially slumped case is therefore not considered separately.

6.4.2   Drift Scenarios (Calculation Set B)

Next, various drift scenarios are considered (Calculation Set B). The events included in the drift scenario subset are:

- Magma cools
- Magma fractures
- Seepage returns

To treat these events, three different drift scenarios are considered: a scenario with molten magma (denoted "hd"), a scenario with cooled and non-fractured magma ("cd"), and a scenario with cooled and fractured magma with seepage filling the fractures ("cw"). As previously stated in Section 6.3.2.5, the case of fractured magma before seepage returns is bounded by non-fractured magma from a criticality standpoint.

All cases run in this subset were run with the most reactive damage configuration (Section 6.4.1). All cases run in this subset were of flow-through configuration 0, representing dry and non-degraded fuel (as described in Section 6.4.3).

The results from Calculation Set B are examined to find the most reactive case in the set. This damage and drift scenario combination is used in the degradation scenario subset (Section 6.4.3). In addition, the results are examined to determine the change in reactivity between the most reactive and least reactive drift scenarios. This difference is labeled Δk_{drift}.

6.4.3   Degradation Scenarios (Calculation Set C)

The next step in examining the criticality response is a subset examining possible degradation scenarios (Calculation Set C). The range of possible degradation scenarios was formalized into the following four configurations:

0. Non-degraded
1. Only fuel degraded (metals non-degraded)
2. Only metal degraded (fuel non-degraded)
3. Both fuel and metal degraded

Each of the four degradation configurations above has two variations: flow-through conditions and bathtub conditions. The flow-through cases correspond to cases where water has been able to enter the DOE standardized SNF canister and degrade the contents. The flow-through cases do not contain any residual water. The bathtub cases are functionally identical to the flow-through cases except that they are fully flooded, and all voids and gaps in the DOE standardized SNF canister are filled with water.

For conservatism, each degraded component was represented as completely degraded (i.e., every atom inside the DOE standardized SNF canister reacts and forms a new compound). This results in the highest amount of moderator in the waste package (the waste package inner and outer barriers are deformed but not degraded, as stated in Assumption 3.2.6).

For criticality calculations with degraded fuel, the uranium in the fuel degrades to schoepite ($UO_3 : 2H_2O$). The degradation products for uranium are identified in the *Geochemistry Model Validation Report: Material Degradation and Release Model* (BSC 2006 [DIRS 176911], Table 6-7). The degradation products for uranium are also identified in the individual chemical degradation calculations (Enrico Fermi: BSC 2003 [DIRS 169107], Section 6; TRIGA: CRWMS M&O 1999 [DIRS 103899], Section 5; FFTF: BSC 2001 [DIRS 157195], Section 6). Of the degradation products identified, schoepite was the most common degradation product and also the degradation product with the highest hydrogen to uranium ratio. For criticality calculations with degraded structural material, aluminum in stainless steel degrades to diaspore (AlOOH). While aluminum may degrade to other products, diasphore was selected because it is thermodynamically the most stable (BSC 2006 [DIRS 176911], Table 6-7) and more likely to be present. Further, diasphore has a high density (Roberts et. al. 1990 [DIRS 107105], p. 226) which makes it more compact and will therefore not exclude as much water as other products (e.g., gibbsite). For the purpose of this calculation, iron in stainless steel degrades to goethite (FeOOH) rather than hematite (Fe_2O_3). Comparisons of goethite and hematite utilizing configurations 2 and 3 were performed with the FFTF fuel, which verified that goethite produces slightly higher k_{eff} values than hematite. The results for hematite are presented in Table 6.4-2 and the results from the calculations using goethite are shown in Table 7.2-3. The material composition of hematite was calculated in *materials.xls*. Each of these transitions mentioned above results in a volume increase due to the change in density from original material to degraded material.

Table 6.4-2. FFTF Results Utilizing Hematite, Scenario Set C (Degradation)

Magma Cooled	Magma Fractures After Cooling	Seepage Returns	Bathtub Config Formed	Waste Form Degraded Config	Case ID	keff	σ	keff + 2σ
Y	Y	Y	N	2	2.H.wcx.cd.f2	0.52486	0.00055	0.52596
Y	Y	Y	Y	2	2.H.wcx.cd.b2	0.76976	0.00086	0.77148
Y	Y	Y	N	3	2.H.wcx.cd.f3	0.49066	0.00066	0.49198
Y	Y	Y	Y	3	2.H.wcx.cd.b3	0.74883	0.00093	0.75069

To accommodate the added volume, new dimensions were determined for each of the waste package components and contents. Voids (from non-degraded packages) were also reduced to bring the waste package materials into closer proximity to the fuel.

Initially, the eight degradation scenarios above (four degradation configurations, each with two variations) are run under the most reactive damage scenario identified in Calculation Set A (Section 6.4.1) and the most reactive drift scenario identified in Calculation Set B (Section 6.4.2). The degradation case with the highest value of k_{eff} is run again with the HLW degraded into clay, which brings the total number of degradation cases up to nine.

The results from Calculation Set C are examined to find the most reactive case in the set. In addition, the results are examined to determine the change in reactivity between the most

reactive and least reactive degradation scenarios. This difference is labeled Δk_{deg}.

It is important to emphasize that a wide range of geometric configurations is possible during the degradation of the waste package contents (see Section 6.3.2.9). The specific cases run were chosen to represent this range. It is expected that this is a bounding set of degradation scenarios for igneous events. However, as mentioned in Section 6.3.2.9, the degraded criticality analyses for each SNF type are the primary source for conclusions regarding degraded configurations. Those analyses feature a more complete range of geometric configurations as well as conservative reflection and moderation conditions, and they are expected to bound any possible igneous scenarios.

6.4.4   Critical Limit Calculations

The methodology for calculating the critical limit along with the actual calculations are described in Attachment I. Enrico Fermi fuel is the only DOE SNF used for the critical limit calculation. The critical limit for the remaining DOE SNF is established per Assumption 3.2.7.

6.5   MATERIAL DESCRIPTIONS

When calculating the degraded compositions in the following section, the densities given in Table 6.5-1 were used for degraded materials.

Table 6.5-1. Density of Various Degradation Products

Material	Density (g/cm^3)	Reference
Schoepite (UO_3:$2H_2O$)	4.8738[a]	DTN: SN0410T0510404.002 [DIRS 172712], file data0.ymp
Goethite (FeOOH)	4.2800	Weast, R.C., ed. 1972 [DIRS 127163], p. B-98
Diaspore (AlOOH)	3.4000	Weast, R.C., ed. 1972 [DIRS 127163], p. B-63

[a] The density was calculated by dividing the molecular weight with the molar volume.

6.5.1   Materials Specific to SNF Types

The fuel types presented in the following subsections are taken from the *Dimension and Material Specification Selection for Use in Criticality Analyses* document (BSC 2006 [DIRS 177193]), unless otherwise is stated.

6.5.1.1 Uranium Metal SNF (N-Reactor)

The Mark 1A fuel element utilized for the N-Reactor calculations is enriched to 1.25% U-235 in the outer tube (DOE 2000 [DIRS 150095], Table 3-1) and there are 48 fuel elements in the canister (DOE 2000 [DIRS 150095], Figure 4-2). The density of the uranium metal is 18.39 g/cm^3 and is calculated in the following manner. The outer fuel tube is 6.096 cm diameter on the outside, 4.496 cm diameter on the inside and it is 53 cm long (DOE 2000 [DIRS 150095], Table 3-1). The cladding is 0.0635 cm thick on the outside and 0.0555 cm thick on the inside (DOE 2000 [DIRS 150095], Table 3-2). Therefore the volume of fuel in the outer tube is [π

$(6.096/2 - 0.0635)^2 - \pi (4.496/2 + 0.0555)^2] \times 53 = 599.61$ cm^3. Similarly, the inner tube is 3.175 cm diameter on the outside, 1.118 cm diameter on the inside and it is 53 cm long (DOE 2000 [DIRS 150095], Table 3-1). The cladding is 0.1015 cm thick on the outside and 0.0635 cm thick on the inside (DOE 2000 [DIRS 150095], Table 3-2). The volume of fuel in the inner tube is then $[\pi (3.175/2 - 0.1015)^2 - \pi (1.118/2 + 0.0635)^2] \times 53 = 303.15$ cm^3. The total volume of uranium metal is then $599.61 + 303.15 = 902.76$ cm^3. The total mass of uranium metal in this fuel element is $11.1 + 5.5 = 16.6$ kg (DOE 2000 [DIRS 150095], Table 3-1). Therefore, the density of the metal is $16600/902.76 = 18.39$ g/cm^3.

6.5.1.2 Mixed Oxide Fuel (Fast Flux Test Facility)

Tables 6.5-2 through 6.5-5 present the fuel composition and Inconel composition used for the FFTF criticality calculations.

Table 6.5-2. Composition and Density of FFTF Type 4.1 Fuel

Intact Fuel ($UO_{1.96}$ / $PuO_{1.96}$)		Degraded Fuel (Schoepite / $PuO_{1.96}$)	
Element / Isotope	Composition (wt%) [a]	Element / Isotope	Composition (wt%) [b]
U-235	0.125	U-235	0.105
U-238	62.373	U-238	52.578
Pu-239	22.595	Pu-239	19.046
Pu-240	3.017	Pu-240	2.543
Pu-241	0.265	Pu-241	0.223
O	11.626	O	24.612
		H	0.892
Material Density	10.02 g/cm^3	Material Density	5.7171 g/cm^3

Sources: [a] BSC 2006 [DIRS 177193], Table 46.
[b] Calculated in Attachment III, file *FFTF.xls*, worksheet "Compositions" using data from Audi and Wapstra 1995 [DIRS 149625], pp. 1, 3, 60, and 61.

Table 6.5-3. Composition and Density of FFTF Ident-69 Fuel Pins

Intact Fuel ($UO_{1.96}$ / $PuO_{1.96}$)		Degraded Fuel (Schoepite / $PuO_{1.96}$)	
Element / Isotope	Composition (wt%) [a]	Element / Isotope	Composition (wt%) [b]
U-235	0.122	U-235	0.103
U-238	60.681	U-238	51.507
Pu-239	24.077	Pu-239	20.437
Pu-240	3.214	Pu-240	2.729
Pu-241	0.282	Pu-241	0.239
O	11.625	O	24.111
		H	0.874
Material Density	10.02 g/cm^3	Material Density	5.7675 g/cm^3

Sources: [a] BSC 2006 [DIRS 177193], Table 47.
[b] Calculated in Attachment III, file *FFTF.xls*, worksheet "Compositions" using Assumption 3.2.8 and data from Audi and Wapstra 1995 [DIRS 149625], pp. 1, 3, 60, and 61.

Table 6.5-4. Composition and Density of Natural UO_2

Intact Fuel (UO_2)		Degraded Fuel (Schoepite)	
Element / Isotope	Composition (wt%) [a]	Element / Isotope	Composition (wt%) [b]
U-235	0.640	U-235	0.536
U-238	87.510	U-238	73.373
O	11.850	O	24.839
		H	1.252
Material Density	10.42 g/cm^3	Material Density	4.8738 g/cm^3

Sources: [a] BSC 2006 [DIRS 177193], Table 48.
[b] Calculated in Attachment III, file *FFTF.xls*, worksheet "Compositions" using data from Audi and Wapstra 1995 [DIRS 149625], pp. 1, 3, 60, and 61.

Table 6.5-5. Composition and Density of Inconel 600 (UNS N06600)

Isotope / Element	Composition (wt%) [a]	Value Used (wt%)
C	0.15 (max)	0.150
Mn	1.0 (max)	1.000
S	0.015 (max)	0.015
Si	0.5 (max)	0.500
Cu	0.5 (max)	0.500
Cr	14 to 17	15.500
Fe	6 to 10	8.000
Ni	Balance	73.835
Material Density	8.47 g/cm^3	8.4700 g/cm^3

Source: [a] Inco Alloys International 1988 [DIRS 130835], p. 9.

6.5.1.3 U-Mo / U-Zr SNF (Enrico Fermi Fast Reactor)

Zirconium with a density of 6.506 g/cm^3 (Weast, R.C., ed. 1972 DIRS [127163], p B-38) was used for the cladding of the Fermi fuel. Tables 6.5-6 and 6.5-7 present the fuel and Fe/GdPO$_4$ shot composition and density used in the criticality calculations.

Table 6.5-6. Composition and Density of Fermi Fuel

Intact Fuel (U/Mo)		Degraded Fuel and Clad (Schoepite, Mo, Zr)	
Element / Isotope	Composition (wt%) [a]	Element / Isotope	Composition (wt%) [b]
U-235	22.961	U-235	16.663
U-238	66.413	U-238	48.198
Mo	10.625	O	21.868
		H	1.102
		Mo	7.711
		Zr	4.457
Material Density	17.4242 g/cm^3	Material Density	5.1385 g/cm^3

Sources: [a] BSC 2006 [DIRS 177193], Table 35 and Assumption 3.2.10.
   [b] Calculated in Attachment III, file *Fermi.xls* using data from Audi & Wapstra 1995 [DIRS 149625], pp. 1-65.

Table 6.5-7. Composition and Density of Fe / $GdPO_4$ Shot

Vol% $GdPO_4$	Flowthrough Config (Intact, Dry) [a]			Bathtub Config (Intact, Flooded) [a]			Degraded Config [a]		
	0%	3%	9%	0%	3%	9%	0%	3%	9%
Fe	100.000	98.074	94.091	91.835	89.985	86.169	62.853	62.086	60.466
Gd-152	---	0.002	0.007	---	0.002	0.007	---	0.001	0.005
Gd-154	---	0.026	0.079	---	0.024	0.072	---	0.016	0.051
Gd-155	---	0.175	0.537	---	0.161	0.492	---	0.111	0.345
Gd-156	---	0.244	0.748	---	0.224	0.685	---	0.154	0.481
Gd-157	---	0.188	0.575	---	0.172	0.527	---	0.119	0.370
Gd-158	---	0.300	0.919	---	0.275	0.842	---	0.190	0.591
Gd-160	---	0.267	0.819	---	0.245	0.750	---	0.169	0.526
P	---	0.237	0.726	---	0.217	0.665	---	0.150	0.466
O	---	0.489	1.499	7.252	7.774	8.850	36.013	35.883	35.609
H	---	---	---	0.914	0.923	0.942	1.134	1.121	1.091
Material Density	4.6315 g/cm^3	4.5808 g/cm^3	4.4793 g/cm^3	5.0433 g/cm^3	4.9926 g/cm^3	4.8911 g/cm^3	4.2800 g/cm^3	4.2875 g/cm^3	4.3035 g/cm^3

Source: [a] Calculated in Attachment III, file *Fermi.xls*, worksheet "Fe-Gd-H2O" using data from CRWMS M&O 1999 [DIRS 104118], Attachment VI, Audi & Wapstra 1995 [DIRS 149625], pp. 1-65, Weast, R.C., ed. 1972 [DIRS 127163], p. B-18 and B-98), and Assumption 3.2.11.

6.5.1.4 Highly-Enriched Uranium Oxide SNF (Shippingport PWR)

The fuel is a mixture of UO_2-ZrO_2-CaO with varying reactivity divided into three zones. Table 6.5-8 shows the various fuel compositions and densities used in the criticality calculations.

Table 6.5-8. Composition and Density of Shippingport PWR Fuel

Zone 1		Zone 2		Zone 3	
Element / Isotope	Composition (wt%) [a,b]	Element / Isotope	Composition (wt%) [b]	Element / Isotope	Composition (wt%) [b]
U-235	45.04	U-235	32.98	U-235	21.74
U-238	3.29	U-238	2.41	U-238	1.59
Zr	29.54	Zr	39.98	Zr	49.68
Ca	3.72	Ca	4.15	Ca	4.57
O	18.42	O	20.49	O	22.42
Material Density	6.36 g/cm^3	Material Density	5.79 g/cm^3	Material Density	5.35 g/cm^3

Sources: [a] BSC 2006 [DIRS 177193], Section 6.3.2.6.
   [b] Calculated in Attachment III, file *Shippingport.xls*, with fuel matrix compositions for zones 1, 2, and 3 from DOE 1999 [DIRS 104940], Table 3-2.

6.5.1.5 Uranium / Thorium Oxide SNF (Shippingport LWBR)

The fuel consists of a binary matrix of UO_2-ThO_2. The core is divided into a high enrichment zone and a low enrichment zone with a ThO_2 reflector region above and below the fuel regions. Table 6.5-9 shows the various fuel compositions and densities used in the criticality calculations.

Table 6.5-9. Composition and Density of Shippingport LWBR Fuel

High Enrichment Zone		Low Enrichment Zone	
Element / Isotope	Composition (wt%) [a]	Element / Isotope	Composition (wt%) [a, b]
Th-232	83.28	Th-232	84.05
U-233	4.57	U-233	3.81
U-234	0.06	U-234	0.05
U-235	0.00	U-235	0.00
U-236	0.00	U-236	0.00
U-238	0.02	U-238	0.01
O	12.07	O	12.07
Material Density	9.71 g/cm³	Material Density	9.665 g/cm³

Sources: [a] BSC 2006 [DIRS 177193], Section 6.3.2.5.
[b] Calculated in Attachment III, file *Shippingport.xls*.

6.5.1.6 Graphite / Carbide SNF (Ft. St. Vrain)

Fort St. Vrain (FSV) fuel consists of small particles of uranium carbide, which are coated with pyrolytic carbon and silicon carbide and then bound in a carbonized matrix to form a solid substance. Table 6.5-10 displays the composition and density of Fort St. Vrain fuel.

Table 6.5-10. Composition and Density of FSV Fuel

Intact Fuel (Graphite/Carbide Matrix)	
Element / Isotope	Composition (wt%) [a,b]
U-235	3.535
Th-232	25.689
Si	5.962
C	64.808
Pu-239	0.006
Material Density	1.9911 g/cm³

Sources: [a] BSC 2006 [DIRS 177193], Section 6.3.2.2.
[b] Calculated in Attachment III, file *FSV.xls*, worksheet "Compositions".

6.5.1.7 U-Zr-Hx SNF (TRIGA Reactor)

Table 6.5-11 presents the composition and density of TRIGA fuel used in the criticality calculations.

Table 6.5-11. Composition and Density of TRIGA Fuel

Intact Fuel (U70ZrH1.6)		Degraded Fuel (Schoepite, H, Zr)	
Element / Isotope	Composition (wt%) [a]	Element / Isotope	Composition (wt%) [b]
U-235	5.940	U-235	5.765
U-238	2.558	U-238	2.483
Zr	89.911	Zr	87.269
H	1.591	H	1.685
		O	2.797
Material Density	5.9832 g/cm^{3} [b]	Material Density	5.5421 g/cm^3

Sources: [a] BSC 2006 [DIRS 177193], Section 6.3.2.1 and Assumption 3.2.12.
            [b] Calculated in Attachment III, file *TRIGA.xls*, worksheet "Compositions" using data from Audi and Wapstra
                1995 [DIRS 149625], pp. 1, 3, 60, and 61.

6.5.1.8 Aluminum-Based SNF (Advanced Test Reactor)

Table 6.5-12 displays the composition and density of intact ATR fuel.

Table 6.5-12. Composition and Density of Intact ATR Fuel

Intact Fuel (U/Al$_x$ in Al matrix)			
Element / Isotope	Composition of Plates 1, 2, 18, and 19 (wt%) [a,b]	Composition of Plates 3, 4, 16, and 17 (wt%) [a,b]	Composition of Plates 5 through 15 (wt%) [a,b]
U-235	26.505	31.056	35.671
U-238	1.692	1.982	2.277
Al	71.539	66.732	61.857
Si	0.143	0.125	0.106
Cu	0.115	0.100	0.085
Cd	0.001	0.001	0.001
Li-7	0.004	0.004	0.003
Material Density	3.5378 g/cm^3	3.7611 g/cm^3	4.0183 g/cm^3

Sources: [a] BSC 2006 [177193], Table 39.
            [b] Calculated in Attachment III, file *ATR.xls*, worksheet "Intact Fuel" using data from Parrington, J.R., et. al.
                1996 [DIRS 103896], pp. 1-64.

6.5.1.9 Low-Enriched Uranium Oxide (Three Mile Island)

Table 6.5-13 presents the composition and density for TMI fuel used in the criticality calculations.

Table 6.5-13. Composition and Density of TMI Fuel

Intact Fuel (UO$_2$, 2.96% enriched)		Degraded Fuel (Schoepite, 2.96% enriched)	
Element / Isotope	Composition (wt%) [a]	Element / Isotope	Composition (wt%) [b]
U-235	2.609	U-235	2.188
U-238	85.538	U-238	71.716
O	11.853	O	24.845
		H	1.252
Material Density	10.4215 g/cm^3	Material Density	4.8738 g/cm^3

Sources: [a] BSC 2006 [DIRS 177193], Table 42.
         [b] Calculated in Attachment III, file *TMI.xls*, worksheet "Compositions".

6.5.2   Structural Materials

Tables 6.5-14 through 6.5-20 display the composition and density of structural materials used in the criticality calculations.

Table 6.5-14. Composition and Density of Aluminum 6061 (UNS A96061)

Isotope / Element	Composition (wt%) [a]	Composition, Intact Conditions (wt%) [a]	Composition, Degraded Conditions (Gibbsite, wt%) [b]
Si	0.4 to 0.8	0.600	0.275
Fe	0.7 (max)	0.700	0.320
Cu	0.15 to 0.4	0.275	0.126
Mn	0.15 (max)	0.150	0.069
Mg	0.8 to 1.2	1.000	0.458
Cr	0.04 to 0.35	0.195	0.089
Zn	0.25 (max)	(added to Al) [c]	---
Ti	0.15 (max)	0.150	0.069
Residuals	0.15 (max)	(added to Al)	---
Al	Balance	96.930	44.346
O	---	---	52.593
H	---	---	1.657
Material Density	2.713 [a] g/cm^3	2.7100 g/cm^3	3.3879 g/cm^3

Sources: [a] BSC 2006 [DIRS 177193], Table 8.
         [b] Calculated in Attachment III, file *materials.xls,* worksheet "UNS A96061" using data from Audi and Wapstra 1995 [DIRS 149625], pp. 1-65.

NOTE: [c] See Assumption 3.2.3.

Table 6.5-15. Composition and Density of A 516 Carbon Steel, Grade 70 (UNS K02700)

Isotope / Element	Composition (wt%) [a]	Value Used, Intact Conditions (wt%)	Value Used, Degraded Conditions (Goethite, wt%) [c]
C	0.28 (½ in to 2 in thick)	0.280	0.177
Mn	0.85 to 1.20 (over ½ in)	1.025	0.648
P	0.035	0.035	0.022
S	0.035	0.035	0.022
Si	0.15 to 0.40	0.275	0.174
Fe	Balance	98.350	62.197
O	---	---	35.637
H	---	---	1.123
Material Density	7.850 g/cm^3 [b]	7.8500 g/cm^3	4.3004 g/cm^3

Sources: [a] ASTM A 516/A 516M-90 1991 [DIRS 117138], p. 2, Table 1 except where noted.
      [b] ASME 2001 [DIRS 158115], Section II-A, SA-20, Section 14.1.
      [c] Calculated in Attachment III, file *materials.xls*, worksheet "UNS K02700" using data from Audi and Wapstra 1995 [DIRS 149625], pp. 1-65.

Table 6.5-16. Composition and Density of Alloy 22 (UNS N06022)

Isotope / Element	Composition (wt%) [a]	Value Used (wt%)
C	0.015 (max)	0.015
Mn	0.50 (max)	0.500
Si	0.08 (max)	0.080
Cr	20.0 to 22.5	21.250
Mo	12.5 to 14.5	13.500
Co	2.50 (max)	2.500
W	2.5 to 3.5	3.000
V	0.35 (max)	0.350
Fe	2.0 to 6.0	4.000
P	0.02 (max)	0.020
S	0.020 (max)	0.020
Ni	Balance	54.765
Material Density	8.690 g/cm^3	8.690 g/cm^3

Source: [a] DTN: MO0003RIB00071.000 [DIRS 148850].

Table 6.5-17. Composition and Density of Ni-Gd Alloy (UNS N06464)

Isotope / Element	Composition (wt%) [a]	Value Used (wt%)	Isotope / Element	Composition (wt%) [a]	Value Used (wt%)
Mo	13.1 to 16.0	14.550	O	0.005	0.005
Cr	14.5 to 17.1	15.800	Ni	Remainder	64.535
Fe	1.0 (max)	1.000	Gd	1.9 to 2.1	1.500 [b]
Co	2.0 (max)	2.000			Gd-152	0.003
C	0.010 (max)	0.010			Gd-154	0.032
Si	0.08 (max)	0.080			Gd-155	0.219
Mn	0.5 (max)	0.500			Gd-156	0.304
P	0.005 (max)	0.005			Gd-157	0.234
S	0.005 (max)	0.005			Gd-158	0.374
N	0.010 (max)	0.010			Gd-160	0.334
Material density 8.76 g/cm^3 [a]					

Source: [a] ASTM B 932-04 2004 [DIRS 168403], Table 1.

NOTES: [b] 1.5 wt% Gd is based on typical value of 75% credit (NRC 2000 [DIRS 149756], p. 8-4) allowed for fixed neutron absorbers and a nominal Gd loading of 2.0 wt%

Table 6.5-18. Composition and Density of SS 304L (UNS S30403)

Isotope / Element	Composition (wt%) [a]	Value Used, Intact Conditions (wt%)	Value Used, Degraded Conditions (Goethite, wt%) [b]
C	0.03 (max)	0.030	0.021
Mn	2.0 (max)	2.000	1.426
P	0.045 (max)	0.045	0.032
S	0.03 (max)	0.030	0.021
Si	0.75 (max)	0.750	0.535
Cr	18 to 20	19.000	13.551
Ni	8 to 12	10.000	7.132
N	0.10	0.100	0.071
Fe	Balance	68.045	48.529
O	---	---	27.806
H	---	---	0.876
Material Density	7.940 g/cm^3	7.940 g/cm^3	4.7824 g/cm^3

Source: [a] ASME (2001 [DIRS 158115], Section II, SA-240, Table 1); density from ASTM (1999 [DIRS 103515], G 1-90, p. 7, Table X1).
         [b] Calculated in Attachment III, file *materials.xls*, worksheet "UNS S30403" using data from Audi and Wapstra 1995 [DIRS 149625], pp. 1-65.

Table 6.5-19. Composition and Density of SS 316 Nuclear Grade (UNS S31600)

Isotope / Element	Composition (wt%) [a]	Value Used, Intact Conditions (wt%)	Value Used, Degraded Conditions (Goethite, wt%) [d]
C	0.020 (max) [b]	0.020	0.014
Mn	2.00 (max)	2.000	1.441
P	0.045 (max)	0.045	0.032
S	0.03 (max)	0.030	0.022
Si	0.75 (max)	0.750	0.541
Cr	16.00 to 18.00	17.000	12.252
Ni	10.00 to 14.00	12.000	8.648
Mo	2.00 to 3.00	2.500	1.802
N	0.060 – 0.100 [b]	0.080	0.058
Fe	Balance	65.575	47.259
O	---	---	27.078
H	---	---	0.853
Material Density	7.980 g/cm^3 [c]	7.980 g/cm^3	4.8363 g/cm^3

Sources: [a] Source data from (ASME 2001 [DIRS 158115], Section II, SA-240, Table 1) except where specified.
   [b] Source data from (ASM International 1987 [DIRS 133378], p. 931).
   [c] Density for SS 316 used. Data taken from (BSC 2006 [DIRS 177193], Table 5).
   [d] Calculated in Attachment III, file *materials.xls*, worksheet "UNS S31600" in each file using data from Audi and Wapstra 1995 [DIRS 149625], pp. 1-65.

Table 6.5-20. Composition and Density of SS 316L (UNS S31603)

Isotope / Element	Composition (wt%) [a]	Value Used, Intact Conditions (wt%)	Value Used, Degraded Conditions (Goethite, wt%) [c]
C	0.03 (max)	0.030	0.022
Mn	2.00 (max)	2.000	1.443
P	0.045 (max)	0.045	0.032
S	0.03 (max)	0.030	0.022
Si	1.00 (max)	1.000	0.722
Cr	16.00 to 18.00	17.000	12.266
Ni	10.00 to 14.00	12.000	8.659
Mo	2.00 to 3.00	2.500	1.804
N	0.10 (max)	0.100	0.072
Fe	Balance	65.295	47.114
O	---	---	26.995
H	---	---	0.850
Material Density	7.980 g/cm^3 [b]	7.9800 g/cm^3	4.8422 g/cm^3

Sources: [a] ASTM A 276-91a 1991 [DIRS 104133], p. 2, Table 1 except where specified.
   [b] ASTM G 1-90 1999 [DIRS 103515], p. 7, Table X1.
   [c] Calculated in Attachment III, file *materials.xls*, worksheet "UNS S31603" in each file using data from Audi and Wapstra 1995 [DIRS 149625], pp. 1-65.

6.5.3   Reflecting and Moderating Materials

Tables 6.5-21 through 6.5-24 display the density and composition of reflecting and moderating materials. Note that the HLW glass is represented as SRS glass (Assumption 3.1.1). Further, the water content of the molten (non-cooled) magma is 4.0 percent by weight. Magma water content is discussed in detail in *Characterize Eruptive Processes at Yucca Mountain, Nevada* (BSC 2004 [DIRS 169980], Section 6.3.2.2), which states that 4.0 weight percent is an effective upper bound for water content in magma. It is conservative to model the upper water bound.

Table 6.5-21. Composition and Density of Savannah River Site High-Level Waste Glass

Element / Isotope	Composition (wt %) [a]	Element / Isotope	Composition (wt %) [a]
Li-6	9.5955E-02	Cu	1.5264E-01
Li-7	1.3804E+00	Ag	5.0282E-02
B-10	5.9176E-01	Ba-137 [b]	1.1267E-01
B-11	2.6189E+00	Pb	6.0961E-02
O	4.4770E+01	Cl	1.1591E-01
F	3.1852E-02	Th-232	1.8559E-01
Na	8.6284E+00	Cs-133	4.0948E-02
Mg	8.2475E-01	Cs-135	5.1615E-03
Al [c]	2.3318E+00	U-234	3.2794E-04
Si	2.1888E+01	U-235	4.3514E-03
S	1.2945E-01	U-236	1.0415E-03
K	2.9887E+00	U-238	1.8666E+00
Ca	6.6188E-01	Zn [c]	6.4636E-02
Ti	5.9676E-01	Pu-238	5.1819E-03
Mn	1.5577E+00	Pu-239	1.2412E-02
Fe	7.3907E+00	Pu-240	2.2773E-03
Ni	7.3490E-01	Pu-241	9.6857E-04
P	1.4059E-02	Pu-242	1.9168E-04
Cr	8.2567E-02		
Material Density	2.85 g/cm^3 at 25 °C, 2.69 g/cm^3 at 825 °C		

Sources: [a] BSC 2006 [DIRS 177193], Table 19.

NOTES: [b] See Assumption 3.2.4
        [c] See Assumption 3.2.3

Table 6.5-22. Composition of Clayey Material

Element/Isotope	Weight Percent (wt%)	Element/Isotope	Weight Percent (wt%)
Ag	2.8009E-02	Na	4.4492E-02
Al	1.4213E+00	Ni	1.6971E+00
Ba-137	6.8590E-02	O	3.8704E+01
Ca	3.9011E-01	P	1.6405E-02
Cl	9.2057E-03	Pb	3.7193E-02
Cr	3.5428E-02	Pu-238	1.8638E-03
Cu	7.8954E-02	Pu-239	4.4832E-03
F	3.3558E-03	Pu-240	8.2600E-04
Fe	4.1248E+01	Pu-241	3.5278E-04
H	2.6893E-01	Pu-242	7.0105E-05
K	7.2980E-02	Si	1.3588E+01
Mg	2.5328E-01	Th-232	1.1293E-01
Mn	1.5492E+00	Ti	3.6452E-01
Density = 4.23 g/cm^3			

Source: CRWMS M&O 2000 (DIRS [150852]), p. 17 and Attachment V, spreadsheet: "*clayey material pre breach.xls*"(density).

Table 6.5-23. Composition and Density of Magma

Compound	Composition (wt%) Dry Magma [a]	Element / Isotope	Composition (wt%) Dry Magma (4.0 wt% water) [b]	Composition (wt%) Wet Magma (6.20 wt% water) [b]
SiO_2	48.50	H	0.45	0.69
TiO_2	1.93	O	45.93	46.92
Al_2O_3	16.74	Si	21.98	21.48
Fe_2O_3	1.74	Al	8.59	8.39
FeO	8.90	Fe	7.89	7.71
MnO	0.17	Mg	3.41	3.33
MgO	5.83	Ca	5.96	5.82
CaO	8.60	Na	2.54	2.48
Na_2O	3.53	K	1.48	1.45
K_2O	1.84	Ti	1.12	1.10
P_2O_5	1.22	P	0.52	0.50
		Mn	0.13	0.12
		Material Density	2.474 g/ cm^3 [c] (Liquidus)	2.407 g/cm^3 [b] (no seepage)
			2.664 g/cm^3 [b] (25 °C)	2.566 g/cm^3 [b] (with seepage)

Sources: [a] BSC 2004 [DIRS 169980], Table 6-2.
[b] Calculated in Attachment III, file *materials.xls*, worksheets "Dry Magma" and "Wet Magma" using data from Audi and Wapstra 1995 [DIRS 149625], pp. 1-65, Assumption 3.2.5.
[c] BSC 2004 [DIRS 169980], Table 6-4.

Table 6.5-24. Composition and Density of Tuff

Compound	Composition (wt%) Dry Tuff [a]	Element / Isotope	Composition (wt%) Dry Tuff (0 vol% water) [b]	Composition (wt%) Wet Tuff (15.91 vol% water) [b]
SiO_2	76.29	H	0.00	0.79
TiO_2	0.11	O	49.29	52.07
Al_2O_3	12.55	Si	35.96	33.43
Fe_2O_3	0.97	Al	6.70	6.23
FeO	0.14	Fe	0.79	0.74
MnO	0.07	Mg	0.08	0.07
MgO	0.13	Ca	0.36	0.33
CaO	0.50	Na	2.63	2.45
Na_2O	3.52	K	4.04	3.76
K_2O	4.83	Ti	0.07	0.06
P_2O_5	<0.05	P	0.02	0.02
		Mn	0.05	0.05
		Material Density	2.098 g/cm^3 [c]	2.257 g/cm^3 [b]

Sources: [a] DTN: GS000308313211.001 [DIRS 162015], "Mean" values.
    [b] Calculated in Attachment III, file *materials.xls*, worksheets "Dry Tuff" and "Wet Tuff" using data from Audi and Wapstra 1995 [DIRS 149625], pp. 1-65.
    [c] Source data from (DTN: MO0109HYMXPROP.001 [DIRS 155989], Table S01144_001, average of bulk density for all entries with lithostratigraphy values of Tpc, Tpp, or Tpt).

6.6   FORMULAS

6.6.1   Circumference and Area of a Segment of a Circle

Areas of horizontal cylinder segments are used to calculate glass dimensions for slumped cases (Attachment III, file *materials.xls*, worksheet "Glass").

A segment of a circle is the semi-circular area K formed by a chord of length c crossing a circle of radius R. The height of the segment is h and the distance from the circle center to the chord that forms the segment is d. The length of the curved boundary of the segment is s and the circumference is C. The central angle (angle of the circle from one end of the segment to the other) is denoted θ and is measured in radians. The following can then be written (Beyer, W.H., ed. 1987 [DIRS 103805], p. 125):

General relationships:

$$R = h + d \qquad\qquad s = R\theta$$

$$d = R\cos\left(\frac{\theta}{2}\right) \qquad\qquad c = 2R\sin\left(\frac{\theta}{2}\right)$$

Circumference of a segment of a circle:

$$C = s + c = R\theta + 2R\sin\left(\frac{\theta}{2}\right)$$

$$C = 2R\cos^{-1}\left(\frac{d}{R}\right) + 2\sqrt{R^2 - d^2}$$

$$C = 2R\cos^{-1}\left(\frac{R-h}{R}\right) + 2\sqrt{2Rh - h^2}$$

Area of a segment of a circle:

$$K = \frac{1}{2}R^2(\theta - \sin\theta)$$

$$K = R^2\cos^{-1}\left(\frac{d}{R}\right) - (d)\sqrt{R^2 - d^2}$$

$$K = R^2\cos^{-1}\left(\frac{R-h}{R}\right) - (R-h)\sqrt{2Rh - h^2}$$

Given two of the variables above, these equations can be solved iteratively for the remaining variables. Figure 6.6-1 is provided below to clarify the location of the various variables.
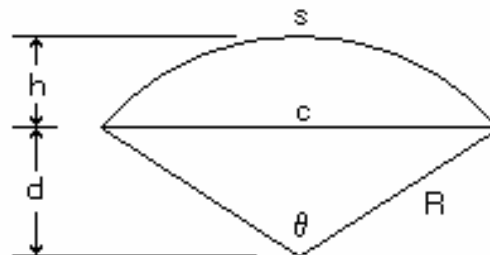
Figure 6.6-1   Description of Variables

6.6.2   Atomic and Mass Weight Percents

The basic equations used to calculate the weight percent values for materials composed of one or more elements/isotopes are shown below. These equations are used in the spreadsheet included in Attachment III, and in the cases described throughout Section 6.

The atomic weights of each isotope are taken from the *Atomic Mass Adjustment, Mass List for Analysis* document (Audi and Wapstra 1995 [DIRS 149625]). The densities and compositions used are listed in Section 5.5 under the appropriate material. Compositions may be specified as atom fractions, weight fractions, or volume fractions. The atom fraction of component i in the composite mixture c is written as $(af)_{i,c}$, and volume fractions and weight fractions are written in a similar manner. A denotes an atomic weight for the component or mixture, and ρ is the density.

When $(af)_{i,c}$ is known:

$$(wf)_{i,c} = (af)_{i,c} \frac{A_i}{A_c} \qquad A_c = \sum_i \left((af)_{i,c} A_i \right) \qquad \frac{1}{\rho_c} = \sum_i \left(\frac{1}{\rho_i} \frac{(af)_{i,c} A_i}{A_c} \right)$$

except when the composite mixture c is a chemical compound (e.g. $GdPO_4$). In this case, $A_c = \sum_i (n_i A_i)$ where n_i is the number of atoms of element i in the compound and ρ_c is looked up in a standard reference.

When $(vf)_{i,c}$ is known:

$$(wf)_{i,c} = (vf)_{i,c} \frac{\rho_i}{\rho_c} \qquad \frac{1}{A_c} = \sum_i \left(\frac{(vf)_{i,c} \rho_i}{A_i \rho_c} \right) \qquad \rho_c = \sum_i \left((vf)_{i,c} \rho_i \right)$$

When $(wf)_{i,c}$ is known:

$$(wf)_{i,c} = (wf)_{i,c} \qquad \frac{1}{A_c} = \sum_i \left(\frac{1}{A_i} (wf)_{i,c} \right) \qquad \frac{1}{\rho_c} = \sum_i \left(\frac{1}{\rho_i} (wf)_{i,c} \right)$$

7. RESULTS AND CONCLUSIONS

This section presents the DOE SNF results for the various calculation sets described in Section 6.4. Per description in Section 6.2, all nine representative DOE fuel types were considered for Calculation Set A (Damage scenarios) and Calculation Set B (Drift scenarios), but only FFTF, Enrico Fermi, TRIGA, and TMI SNF were considered for Calculation Set C (Degradation Scenarios), per explanation in Section 6.2.

7.1   N-REACTOR CRITICALITY RESULTS

7.1.1   Calculation Set A – Damage Scenarios

Table 7.1-1 presents the k_{eff} values for N-Reactor SNF for various damage scenarios outlined in Section 6.4.1. The most conservative (highest) value of $k_{eff} + 2\sigma$ occurs for the 'xcx' configuration. The value of Δk_{damage} is 0.06544 (0.33835 - 0.27291 = 0.06544).

Table 7.1-1. N-Reactor Results, Scenario Set A (Damage)

Waste Package Destroyed	Waste Package Slumps and Breaches	Magma Intrusion into Waste Package	Case ID	k_{eff}	σ	$k_{eff} + 2\sigma$
N	Intact	N	1.A.wig.hd.f0	0.27291	0.00030	0.27351
N	Partial	N	1.A.wpg.hd.f0	0.27493	0.00031	0.27555
N	Partial	Y	1.A.wpx.hd.f0	0.33150	0.00040	0.33230
N	Complete	N	1.A.wcg.hd.f0	0.27552	0.00031	0.27614
N	Complete	Y	1.A.wcx.hd.f0	0.32332	0.00033	0.32398
Y	Partial	N	1.A.xpg.hd.f0	0.27696	0.00029	0.27754
Y	Complete	N	1.A.xcg.hd.f0	0.28020	0.00031	0.28082
Y	Complete	Y	1.A.xcx.hd.f0	0.33835	0.00038	0.33911

7.1.2   Calculation Set B – Drift Scenarios

Table 7.1-2 presents the k_{eff} values for N-Reactor SNF for various drift scenarios (see Section 6.4.2). The most conservative (highest) value of $k_{eff} + 2\sigma$ occurs for the 'cd' configuration. The value of Δk_{drift} is 0.00154 (0.33930 - 0.33776 = 0.00154).

Table 7.1-2. N-Reactor Results, Scenario Set B (Drift)

Magma Cooled	Magma Fractures After Cooling	Seepage Returns	Case ID	k_{eff}	σ	$k_{eff} + 2\sigma$
N	-	-	1.B.xcx.hd.f0	0.33835	0.00038	0.33911
Y	N	-	1.B.xcx.cd.f0	0.33930	0.00040	0.34010
Y	Y	Y	1.B.xcx.cw.f0	0.33776	0.00039	0.33854

7.2   FAST FLUX TEST FACILITY CRITICALITY RESULTS

7.2.1   Calculation Set A – Damage Scenarios

Table 7.2-1 presents the k_{eff} values for FFTF SNF for various damage scenarios outlined in Section 6.4.1. The most conservative (highest) value of $k_{eff} + 2\sigma$ occurs for the 'wcx' configuration. The value of Δk_{damage} is 0.04853 (0.47699 – 0.42846 = 0.04853).

Table 7.2-1. Fast Flux Test Facility Results, Scenario Set A (Damage)

Waste Package Destroyed	Waste Package Slumps and Breaches	Magma Intrusion into Waste Package	Case ID	k_{eff}	σ	$k_{eff} + 2\sigma$
N	Intact	N	2.A.wig.hd.f0	0.43067	0.00039	0.43145
N	Partial	N	2.A.wpg.hd.f0	0.43914	0.00042	0.43998
N	Partial	Y	2.A.wpx.hd.f0	0.47223	0.00055	0.47333
N	Complete	N	2.A.wcg.hd.f0	0.44366	0.00044	0.44454
N	Complete	Y	2.A.wcx.hd.f0	0.47699	0.00051	0.47801
Y	Partial	N	2.A.xpg.hd.f0	0.43272	0.00044	0.43360
Y	Complete	N	2.A.xcg.hd.f0	0.42846	0.00044	0.42934
Y	Complete	Y	2.A.xcx.hd.f0	0.47329	0.00054	0.47437

7.2.2   Calculation Set B – Drift Scenarios

Table 7.2-2 presents the k_{eff} values for FFTF SNF for various drift scenarios (see Section 6.4.2). The most conservative (highest) value of $k_{eff} + 2\sigma$ occurs for the 'cd' configuration. The value of Δk_{drift} is 0.01521 (0.48038 – 0.46517 = 0.01521).

Table 7.2-2. Fast Flux Test Reactor Results, Scenario Set B (Drift)

Magma Cooled	Magma Fractures After Cooling	Seepage Returns	Case ID	k_{eff}	σ	$k_{eff} + 2\sigma$
N	-	-	2.B.wcx.hd.f0	0.47699	0.00051	0.47801
Y	N	-	2.B.wcx.cd.f0	0.48038	0.00051	0.48140
Y	Y	Y	2.B.wcx.cw.f0	0.46517	0.00053	0.46623

7.2.3   Calculation Set C – Degradation Scenarios

Table 7.2-3 presents the k_{eff} values for FFTF SNF for various degradation scenarios outlined in Section 5.4.3. The most conservative (highest) value of $k_{eff} + 2\sigma$ occurs for the 'wcx' bathtub degraded configuration 3. The value of Δk_{deg} is 0.32174 (0.77406 - 0.45232 = 0.32174). The

'wcx' bathtub degraded configuration 3 was also evaluated with the HLW glass region substituted for clay to investigate the more reactive configuration.

Table 7.2-3. Fast Flux Test Reactor Results, Scenario Set C (Degradation)

Magma Cooled	Magma Fractures After Cooling	Seepage Returns	Bathtub Config Formed	Waste Form Degraded Config	Case ID	k_{eff}	σ	$k_{eff} + 2\sigma$
Y	Y	Y	N	0	2.C.wcx.cd.f0	0.48038	0.00051	0.48140
Y	Y	Y	Y	0	2.C.wcx.cd.b0	0.73750	0.00090	0.73930
Y	Y	Y	N	1	2.C.wcx.cd.f1	0.74993	0.00077	0.75147
Y	Y	Y	Y	1	2.C.wcx.cd.b1	0.80051	0.00091	0.80233
Y	Y	Y	N	2	2.C.wcx.cd.f2	0.53151	0.00060	0.53271
Y	Y	Y	Y	2	2.C.wcx.cd.b2	0.77406	0.00089	0.77584
Y	Y	Y	N	3	2.C.wcx.cd.f3	0.73055	0.00080	0.73215
Y	Y	Y	Y	3	2.C.wcx.cd.b3	0.81045	0.00091	0.81227
Y	Y	Y	Y	3 [a]	2.C.wcx.cd.v	0.81213	0.00090	0.81393

NOTE: [a] This is the most reactive degradation case but with the HLW glass region degraded to clay.

7.3   ENRICO FERMI CRITICALITY RESULTS

7.3.1   Calculation Set A – Damage Scenarios

Table 7.3-1 presents the k_{eff} values for Enrico Fermi SNF for various damage scenarios outlined in Section 6.4.1. The most conservative (highest) value of $k_{eff} + 2\sigma$ occurs for the 'wcg' configuration. The value of Δk_{damage} is 0.02390 ((0.50066 – 0.47676) = 0.02390).

Table 7.3-1. Enrico Fermi Results, Scenario Set A (Damage)

Waste Package Destroyed	Waste Package Slumps and Breaches	Magma Intrusion into Waste Package	Case ID	k_{eff}	σ	$k_{eff} + 2\sigma$
N	Intact	N	3.A.wig.hd.f0	0.49077	0.00042	0.49161
N	Partial	N	3.A.wpg.hd.f0	0.49782	0.00044	0.49870
N	Partial	Y	3.A.wpx.hd.f0	0.48552	0.00051	0.48654
N	Complete	N	3.A.wcg.hd.f0	0.50066	0.00046	0.50158
N	Complete	Y	3.A.wcx.hd.f0	0.49373	0.00046	0.49465
Y	Partial	N	3.A.xpg.hd.f0	0.48598	0.00047	0.48692
Y	Complete	N	3.A.xcg.hd.f0	0.47751	0.00045	0.47841
Y	Complete	Y	3.A.xcx.hd.f0	0.47676	0.00047	0.47770

7.3.2   Calculation Set B – Drift Scenarios

Table 7.3-2 presents the k_{eff} values for Enrico Fermi SNF for various drift scenarios (see Section 6.4.2). The most conservative (highest) value of $k_{eff} + 2\sigma$ occurs for the 'cd' configuration. The value of Δk_{drift} is 0.00522 (0.50179 – 0.49657) = 0.00522).

Table 7.3-2. Enrico Fermi Results, Scenario Set B (Drift)

Magma Cooled	Magma Fractures After Cooling	Seepage Returns	Case ID	k_{eff}	σ	$k_{eff} + 2\sigma$
N	-	-	3.B.wcg.hd.f0	0.50066	0.00046	0.50158
Y	N	-	3.B.wcg.cd.f0	0.50179	0.00044	0.50267
Y	Y	Y	3.B.wcg.cw.f0	0.49657	0.00045	0.49747

7.3.3   Calculation Set C – Degradation Scenarios

Table 7.3-3 presents the k_{eff} values for Enrico Fermi SNF for various drift scenarios outlined in Section 6.4.3. The most conservative (highest) value of $k_{eff} + 2\sigma$ occurs for the 'wcg' flow-through degraded configuration 1. The value of Δk_{deg} is 0.40551 (0.78291 - 0.37740= 0.40551). The 'wcg' flow-through degraded configuration 1 was also evaluated with the HLW glass region substituted for clay to investigate the more reactive configuration (see last entry/line in Table 7.3-3).

Table 7.3-3. Enrico Fermi Results, Scenario Set C (Degradation)

Magma Cooled	Magma Fractures After Cooling	Seepage Returns	Bathtub Config Formed	Waste Form Degraded Config	Case ID	k_{eff}	σ	$k_{eff} + 2\sigma$
Y	Y	Y	N	0	3.C.wcg.cd.f0	0.50179	0.00044	0.50267
Y	Y	Y	Y	0	3.C.wcg.cd.b0	0.78291	0.00083	0.78457
Y	Y	Y	N	1	3.C.wcg.cd.f1	0.91540	0.00086	0.91712
Y	Y	Y	Y	1	3.C.wcg.cd.b1	0.91507	0.00088	0.91683
Y	Y	Y	N	2	3.C.wcg.cd.f2	0.63248	0.00068	0.63384
Y	Y	Y	Y	2	3.C.wcg.cd.b2	0.72244	0.00083	0.72410
Y	Y	Y	N	3	3.C.wcg.cd.f3	0.87410	0.00090	0.87590
Y	Y	Y	Y	3	3.C.wcg.cd.b3	0.87420	0.00084	0.87588
Y	Y	Y	N	1 [a]	3.C.wcg.cd.v	0.91321	0.00090	0.91501

NOTE: [a] This is the most reactive degradation case but with the HLW glass region degraded to clay.

7.4 SHIPPINGPORT PWR CRITICALITY RESULTS

7.4.1 Calculation Set A – Damage Scenarios

Table 7.4-1 presents the k_{eff} values for Shippingport PWR SNF for various damage scenarios outlined in Section 6.4.1. The most conservative (highest) value of $k_{eff} + 2\sigma$ occurs for the 'xcx' configuration. The value of Δk_{damage} is 0.06970 ((0.15584 – 0.08614) = 0.06970).

Table 7.4-1. Shippingport PWR Results, Scenario Set A (Damage)

Waste Package Destroyed	Waste Package Slumps and Breaches	Magma Intrusion into Waste Package	Case ID	k_{eff}	σ	$k_{eff} + 2\sigma$
N	Intact	N	4.A.wig.hd.f0	0.08614	0.00014	0.08642
N	Partial	N	4.A.wpg.hd.f0	0.08988	0.00014	0.09016
N	Partial	Y	4.A.wpx.hd.f0	0.15119	0.00037	0.15193
N	Complete	N	4.A.wcg.hd.f0	0.09207	0.00016	0.09239
N	Complete	Y	4.A.wcx.hd.f0	0.14305	0.00033	0.14371
Y	Partial	N	4.A.xpg.hd.f0	0.09228	0.00018	0.09264
Y	Complete	N	4.A.xcg.hd.f0	0.09740	0.00021	0.09782
Y	Complete	Y	4.A.xcx.hd.f0	0.15584	0.00037	0.15658

7.4.2 Calculation Set B – Drift Scenarios

Table 7.4-2 presents the k_{eff} values for Shippingport PWR SNF for various drift scenarios (see Section 6.4.2). The most conservative (highest) value of $k_{eff} + 2\sigma$ occurs for the 'cd' configuration. The value of Δk_{drift} is 0.00809 (0.15809 – 0.15000) = 0.00809).

Table 7.4-2. Shippingport PWR Results, Scenario Set B (Drift)

Magma Cooled	Magma Fractures After Cooling	Seepage Returns	Case ID	k_{eff}	σ	$k_{eff} + 2\sigma$
N	-	-	4.B.xcx.hd.f0	0.15584	0.00037	0.15658
Y	N	-	4.B.xcx.cd.f0	0.15809	0.00039	0.15887
Y	Y	Y	4.B.xcx.cw.f0	0.15000	0.00036	0.15072

7.5   SHIPPINGPORT LWBR CRITICALITY RESULTS

7.5.1   Calculation Set A – Damage Scenarios

Table 7.5-1 presents the k_{eff} values for Shippingport LWBR SNF for various damage scenarios outlined in Section 6.4.1. The most conservative (highest) value of $k_{eff} + 2\sigma$ occurs for the 'xcx' configuration. The value of Δk_{damage} is 0.06171 (0.23091 – 0.16192 = 0.06171).

Table 7.5-1. Shippingport LWBR Results, Scenario Set A (Damage)

Waste Package Destroyed	Waste Package Slumps and Breaches	Magma Intrusion into Waste Package	Case ID	k_{eff}	σ	$k_{eff} + 2\sigma$
N	Intact	N	5.A.wig.hd.f0	0.16192	0.00021	0.16234
N	Partial	N	5.A.wpg.hd.f0	0.16571	0.00020	0.16611
N	Partial	Y	5.A.wpx.hd.f0	0.22655	0.00045	0.22745
N	Complete	N	5.A.wcg.hd.f0	0.16811	0.00023	0.16857
N	Complete	Y	5.A.wcx.hd.f0	0.22201	0.00043	0.22287
Y	Partial	N	5.A.xpg.hd.f0	0.16797	0.00026	0.16849
Y	Complete	N	5.A.xcg.hd.f0	0.17218	0.00029	0.17276
Y	Complete	Y	5.A.xcx.hd.f0	0.23091	0.00045	0.23181

7.5.2   Calculation Set B – Drift Scenarios

Table 7.5-2 presents the k_{eff} values for Shippingport LWBR SNF for various drift scenarios (see Section 6.4.2). The most conservative (highest) value of $k_{eff} + 2\sigma$ occurs for the 'cd' configuration. The value of Δk_{drift} is 0.00845 (0.23250 – 0.22405 = 0.00845).

Table 7.5-2. Shippingport LWBR Results, Scenario Set B (Drift)

Magma Cooled	Magma Fractures After Cooling	Seepage Returns	Case ID	k_{eff}	σ	$k_{eff} + 2\sigma$
N	-	-	5.B.xcx.hd.f0	0.23091	0.00045	0.23181
Y	N	-	5.B.xcx.cd.f0	0.23250	0.00047	0.23344
Y	Y	Y	5.B.xcx.cw.f0	0.22405	0.00046	0.22497

7.6   FORT ST. VRAIN CRITICALITY RESULTS

7.6.1   Calculation Set A – Damage Scenarios

Table 7.6-1 presents the k_{eff} values for Fort St. Vrain SNF for various damage scenarios outlined in Section 6.4.1. The most conservative (highest) value of $k_{eff} + 2\sigma$ occurs for the 'xcx' configuration. The value of Δk_{damage} is 0.11044 (0.19957 – 0.08913 = 0.11044).

Table 7.6-1. For St. Vrain Results, Scenario Set A (Damage)

Waste Package Destroyed	Waste Package Slumps and Breaches	Magma Intrusion into Waste Package	Case ID	k_{eff}	σ	$k_{eff} + 2\sigma$
N	Intact	N	6.A.wig.hd.f0	0.08913	0.00029	0.08971
N	Partial	N	6.A.wpg.hd.f0	0.09553	0.00030	0.09613
N	Partial	Y	6.A.wpx.hd.f0	0.19458	0.00048	0.19554
N	Complete	N	6.A.wcg.hd.f0	0.10334	0.00033	0.10400
N	Complete	Y	6.A.wcx.hd.f0	0.18487	0.00046	0.18579
Y	Partial	N	6.A.xpg.hd.f0	0.09360	0.00031	0.09422
Y	Complete	N	6.A.xcg.hd.f0	0.09849	0.00033	0.09915
Y	Complete	Y	6.A.xcx.hd.f0	0.19957	0.00047	0.20051

7.6.2   Calculation Set B – Drift Scenarios

Table 7.6-2 presents the k_{eff} values for Fort St. Vrain SNF for various drift scenarios (see Section 6.4.2). The most conservative (highest) value of $k_{eff} + 2\sigma$ occurs for the 'cd' configuration. The value of Δk_{drift} is 0.00648 (0.20193 – 0.19545 = 0.00648).

Table 7.6-2. Fort St. Vrain Results, Scenario Set B (Drift)

Magma Cooled	Magma Fractures After Cooling	Seepage Returns	Case ID	k_{eff}	σ	$k_{eff} + 2\sigma$
N	-	-	6.B.xcx.hd.f0	0.19957	0.00047	0.20051
Y	N	-	6.B.xcx.cd.f0	0.20193	0.00047	0.20287
Y	Y	Y	6.B.xcx.cw.f0	0.19545	0.00048	0.19641

7.7 TRIGA REACTOR CRITICALITY RESULTS

7.7.1 Calculation Set A – Damage Scenarios

Table 7.7-1 presents the k_{eff} values for TRIGA SNF for various damage scenarios outlined in Section 6.4.1. The most conservative (highest) value of $k_{eff} + 2\sigma$ occurs for the 'wcx' configuration. The value of Δk_{damage} is 0.01618 (0.47880 – 0.46262 = 0.01618).

Table 7.7-1. TRIGA Reactor Results, Scenario Set A (Damage)

Waste Package Destroyed	Waste Package Slumps and Breaches	Magma Intrusion into Waste Package	Case ID	k_{eff}	σ	$k_{eff} + 2\sigma$
N	Intact	N	7.A.wig.hd.f0	0.46632	0.00073	0.46778
N	Partial	N	7.A.wpg.hd.f0	0.47047	0.00076	0.47199
N	Partial	Y	7.A.wpx.hd.f0	0.46942	0.00073	0.47088
N	Complete	N	7.A.wcg.hd.f0	0.47546	0.00071	0.47688
N	Complete	Y	7.A.wcx.hd.f0	0.47880	0.00069	0.48018
Y	Partial	N	7.A.xpg.hd.f0	0.46495	0.00066	0.46627
Y	Complete	N	7.A.xcg.hd.f0	0.46262	0.00071	0.46404
Y	Complete	Y	7.A.xcx.hd.f0	0.46355	0.00070	0.46495

7.7.2 Calculation Set B – Drift Scenarios

Table 7.7-2 presents the k_{eff} values for TRIGA SNF for various drift scenarios (see Section 6.4.2). The most conservative (highest) value of $k_{eff} + 2\sigma$ occurs for the 'hd' configuration. The value of Δk_{drift} is 0.00972 (0.47880 – 0.46908 = 0.00972). Note that the "hd" and "cd" configurations are statistically identical. For consistency with the other fuel types, the "cd" configuration will be used in Calculation Set C.

Table 7.7-2. TRIGA Reactor Results, Scenario Set B (Drift)

Magma Cooled	Magma Fractures After Cooling	Seepage Returns	Case ID	k_{eff}	σ	$k_{eff} + 2\sigma$
N	-	-	7.B.wcx.hd.f0	0.47880	0.00069	0.48018
Y	N	-	7.B.wcx.cd.f0	0.47803	0.00074	0.47951
Y	Y	Y	7.B.wcx.cw.f0	0.46908	0.00075	0.47058

7.7.3 Calculation Set C – Degradation Scenarios

Table 7.7-3 presents the k_{eff} values for TRIGA SNF for various degradation scenarios outlined in Section 6.4.3. The most conservative (highest) value of $k_{eff} + 2\sigma$ occurs for the 'wcx' bathtub

degraded configuration 3. The value of Δk_{deg} is 0.09413 (0.54320 - 0.44907= 0.09413). The 'wcx' bathtub degraded configuration 3 was also evaluated with the HLW glass region substituted for clay to investigate the more reactive configuration (see last entry/line in Table 7.7-3).

Table 7.7-3. TRIGA Results, Scenario Set C (Degradation)

Magma Cooled	Magma Fractures After Cooling	Seepage Returns	Bathtub Config Formed	Waste Form Degraded Config	Case ID	k_{eff}	σ	$k_{eff} + 2\sigma$
Y	Y	Y	N	0	7.C.wcx.cd.f0	0.47803	0.00074	0.47951
Y	Y	Y	Y	0	7.C.wcx.cd.b0	0.54586	0.00087	0.54760
Y	Y	Y	N	1	7.C.wcx.cd.f1	0.48653	0.00071	0.48795
Y	Y	Y	Y	1	7.C.wcx.cd.b1	0.54234	0.00087	0.54760
Y	Y	Y	N	2	7.C.wcx.cd.f2	0.44907	0.00068	0.45043
Y	Y	Y	Y	2	7.C.wcx.cd.b2	0.53791	0.00086	0.53963
Y	Y	Y	N	3	7.C.wcx.cd.f3	0.46527	0.00072	0.46671
Y	Y	Y	Y	3	7.C.wcx.cd.b3	0.54320	0.00094	0.54508
Y	Y	Y	Y	3 [a]	7.C.wcx.cd.v	0.54665	0.00095	0.54855

NOTE: [a] This is the most reactive degradation case but with the HLW glass region degraded to clay.

7.8   ADVANCED TEST REACTOR CRITICALITY RESULTS

7.8.1   Calculation Set A – Damage Scenarios

Table 7.8-1 presents the k_{eff} values for ATR SNF for various damage scenarios outlined in Section 6.4.1. The most conservative (highest) value of $k_{eff} + 2\sigma$ occurs for the 'xcx' configuration. The value of Δk_{damage} is 0.05816 (0.12255 – 0.06439 = 0.05816).

Table 7.8-1. Advanced Test Reactor Results, Scenario Set A (Damage)

Waste Package Destroyed	Waste Package Slumps and Breaches	Magma Intrusion into Waste Package	Case ID	k_{eff}	σ	$k_{eff} + 2\sigma$
N	Intact	N	8.A.wig.hd.f0	0.06439	0.00011	0.06461
N	Partial	N	8.A.wpg.hd.f0	0.06823	0.00013	0.06849
N	Partial	Y	8.A.wpx.hd.f0	0.11969	0.00027	0.12023
N	Complete	N	8.A.wcg.hd.f0	0.07033	0.00012	0.07057
N	Complete	Y	8.A.wcx.hd.f0	0.11305	0.00025	0.11355
Y	Partial	N	8.A.xpg.hd.f0	0.06899	0.00014	0.06927
Y	Complete	N	8.A.xcg.hd.f0	0.07286	0.00017	0.07320
Y	Complete	Y	8.A.xcx.hd.f0	0.12255	0.00029	0.12313

7.8.2 Calculation Set B – Drift Scenarios

Table 7.8-2 presents the k_{eff} values for ATR SNF for various drift scenarios (see Section 6.4.2). The most conservative (highest) value of $k_{eff} + 2\sigma$ occurs for the 'cd' configuration. The value of Δk_{drift} is 0.00760 (0.12432 – 0.11672 = 0.00760).

Table 7.8-2. Advanced Test Reactor Results, Scenario Set B (Drift)

Magma Cooled	Magma Fractures After Cooling	Seepage Returns	Case ID	k_{eff}	σ	$k_{eff} + 2\sigma$
N	-	-	8.B.xcx.hd.f0	0.12255	0.00029	0.12313
Y	N	-	8.B.xcx.cd.f0	0.12432	0.00029	0.12490
Y	Y	Y	8.B.xcx.cw.f0	0.11672	0.00030	0.11732

7.9 THREE MILE ISLAND CRITICALITY RESULTS

7.9.1 Calculation Set A – Damage Scenarios

Table 7.9-1 presents the k_{eff} values for TMI SNF for various damage scenarios outlined in Section 6.4.1. The most conservative (highest) value of $k_{eff} + 2\sigma$ occurs for the 'wcx' configuration. The value of Δk_{damage} is 0.00995 (0.25803– 0.24808= 0.00995).

Table 7.9-1. Three Mile Island Results, Scenario Set A (Damage)

Waste Package Destroyed	Waste Package Slumps and Breaches	Magma Intrusion into Waste Package	Case ID	k_{eff}	σ	$k_{eff} + 2\sigma$
N	Intact	N	9.A.wig.hd.f0	0.24933	0.00033	0.24933
N	Partial	N	9.A.wpg.hd.f0	0.25142	0.00033	0.25208
N	Partial	Y	9.A.wpx.hd.f0	0.25677	0.00036	0.25749
N	Complete	N	9.A.wcg.hd.f0	0.25195	0.00032	0.25259
N	Complete	Y	9.A.wcx.hd.f0	0.25803	0.00035	0.25873
Y	Partial	N	9.A.xpg.hd.f0	0.24808	0.00034	0.24876
Y	Complete	N	9.A.xcg.hd.f0	0.24816	0.00031	0.24878
Y	Complete	Y	9.A.xcx.hd.f0	0.25509	0.00035	0.25579

7.9.2 Calculation Set B – Drift Scenarios

Table 7.9-2 presents the k_{eff} values for TMI SNF for various drift scenarios (see Section 6.4.2). The most conservative (highest) value of $k_{eff} + 2\sigma$ occurs for the 'cd' configuration. The value of Δk_{drift} is 0.00476 (0.25939 – 0.25463 = 0.00476).

Table 7.9-2. Three Mile Island Results, Scenario Set B (Drift)

Magma Cooled	Magma Fractures After Cooling	Seepage Returns	Case ID	k_{eff}	σ	$k_{eff} + 2\sigma$
N	-	-	9.B.wcx.hd.f0	0.25803	0.00035	0.25873
Y	N	-	9.B.wcx.cd.f0	0.25939	0.00037	0.26013
Y	Y	Y	9.B.wcx.cw.f0	0.25463	0.00036	0.25535

7.9.3   Calculation Set C – Degradation Scenarios

Table 7.9-3 presents the k_{eff} values for TMI SNF for various degradation scenarios outlined in Section 6.4.3. The most conservative (highest) value of $k_{eff} + 2\sigma$ occurs for the 'wcx' bathtub degraded configuration 2. The value of Δk_{deg} is 0.79237 (0.90536 - 0.11299 = 0.79237). The 'wcx' bathtub degraded configuration 2 was also evaluated with the HLW glass region substituted for clay to investigate the more reactive configuration (see last entry/line in Table 7.9-3).

Table 7.9-3. TMI Results, Scenario Set C (Degradation)

Magma Cooled	Magma Fractures After Cooling	Seepage Returns	Bathtub Config Formed	Waste Form Degraded Config	Case ID	k_{eff}	σ	$k_{eff} + 2\sigma$
Y	Y	Y	N	0	9.C.wcx.cd.f0	0.25939	0.00037	0.26013
Y	Y	Y	Y	0	9.C.wcx.cd.b0	0.89285	0.00102	0.89489
Y	Y	Y	N	1	9.C.wcx.cd.f1	0.11299	0.00081	0.11461
Y	Y	Y	Y	1	9.C.wcx.cd.b1	0.36953	0.00045	0.37043
Y	Y	Y	N	2	9.C.wcx.cd.f2	0.36158	0.00056	0.36270
Y	Y	Y	Y	2	9.C.wcx.cd.b2	0.90536	0.00095	0.90726
Y	Y	Y	N	3	9.C.wcx.cd.f3	0.11705	0.00048	0.11801
Y	Y	Y	Y	3	9.C.wcx.cd.b3	0.36934	0.00079	0.37092
Y	Y	Y	Y	2 [a]	9.C.wcx.cd.v	0.90217	0.00098	0.90413

NOTE: [a] This is the most reactive degradation case but with the HLW glass region degraded to clay.

7.10 SUMMARY

Sections 7.1 through 7.9 present the results of parametric evaluations for intact configurations and degraded configurations for the codisposal of DOE SNF. All outputs are reasonable based on the inputs, and the results of this calculation are suitable for their intended use. The results of this calculation are appropriate given the inputs and representations presented throughout this analysis. Variations in geometrical representation and material dimensions and compositions are not considered in this analysis nor are they bounded by the results of this analysis, unless demonstrated.

Based on the results of this calculation and the critical limit in Attachment I, it is concluded that the k_{eff} value of the waste package is less than the critical limit during and after an igneous intrusion event for all DOE SNF designs.

ATTACHMENT I

Determination of the Critical Limit

I.1 INTRODUCTION

As described in the *Disposal Criticality Analysis Methodology Topical Report* (YMP 2003 [DIRS 165505], Section 3.5.2.2), the criticality calculation uses the Monte Carlo method and material cross-section data to evaluate the criticality potential of various configurations. That document also provides basic requirements for validating the calculational method used in a criticality analysis (YMP 2003 [DIRS 165505], Section 3.5.3.2). The bias of a code system (in this case the criticality system containing the Monte Carlo computer code MCNP, selected neutron cross section libraries, and computer hardware) is determined by correlating the results of critical and near-critical experiments with calculated results for those experiments. The common practice, which is used here, is to compare the calculated k_{eff} to that of a critical or near critical system.

An essential element of validating the methods and models used for calculation of k_{eff} is determination of the critical limit (YMP 2003 [DIRS 165505], Section 3.5.3.2.5). For the waste package criticality evaluations, the critical limit is the value of k_{eff} at which a waste package configuration is considered potentially critical. The critical limit is characterized by statistical tolerance limits that account for biases, uncertainties, and limitations. The steps to establish a critical limit are as follows (YMP 2003 [DIRS 165505], Section 3.5.3.2.5):

(1) selection of benchmark experiments;

(2) establishment of the range of applicability of the benchmark experiments (identification of physical and spectral parameters that characterize the benchmark experiments);

(3) establishment of a lower bound tolerance limit; and

(4) establishment of additional uncertainties due to extrapolations or limitations in geometrical or material representations.

I.2 SELECTION OF BENCHMARK EXPERIMENTS

I.2.1 Identifying the Desired Range of Parameters

Before the benchmark experiments can be selected, the operating conditions and parameters for the desired validation must be identified. The fissile isotopes, enrichment of fissile isotopes, fuel density, chemical form of the fuel, types of neutron moderators and reflectors, range of moderator to fissile isotope ratio, neutron absorbers, spectral parameters and physical configurations are among the parameters to specify. These parameters define the area of applicability for the selection of the critical experiments for the validation effort.

The determination of critical limit that follows is based upon the Enrico Fermi waste package, since this was found to be more reactive than the TRIGA fuel (Section 7). The expected scenarios for an igneous intrusion event (Section 6.3) and the subsequent criticality calculation

(Section 6.4 and 7.1) indicated that the most reactive degraded configuration expected is "f1" (degraded fuel but intact structural materials). This geometry is shown in Figure I-1.

A representative case (case "F-f1-9t") was chosen for the critical limit calculation. The MCNP input file for this case was modified to include tally calculations for the neutron flux and fission rate in the mixture containing the fissile material. The input and output files for the critical limit case are *Fcwf1-tr* and *Fcwf1-tr.out* (Attachment III). The resulting neutron flux is calculated in file *Fcwf1-tr_tallies.xls* (Attachment III) and depicted as a function of neutron energy in Figure I-2.
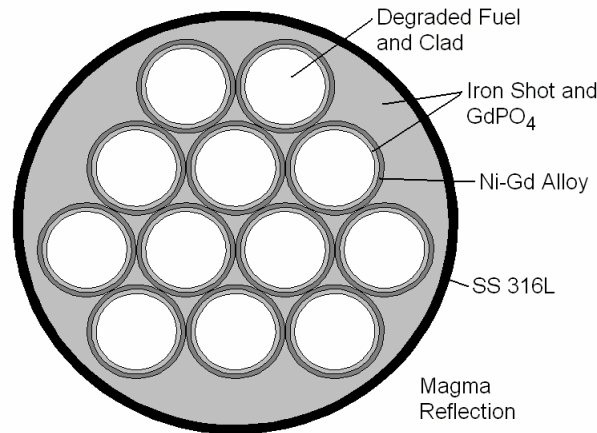

Figure I-1. Radial Cross-sectional View of the Fermi Degraded Configuration "f1"
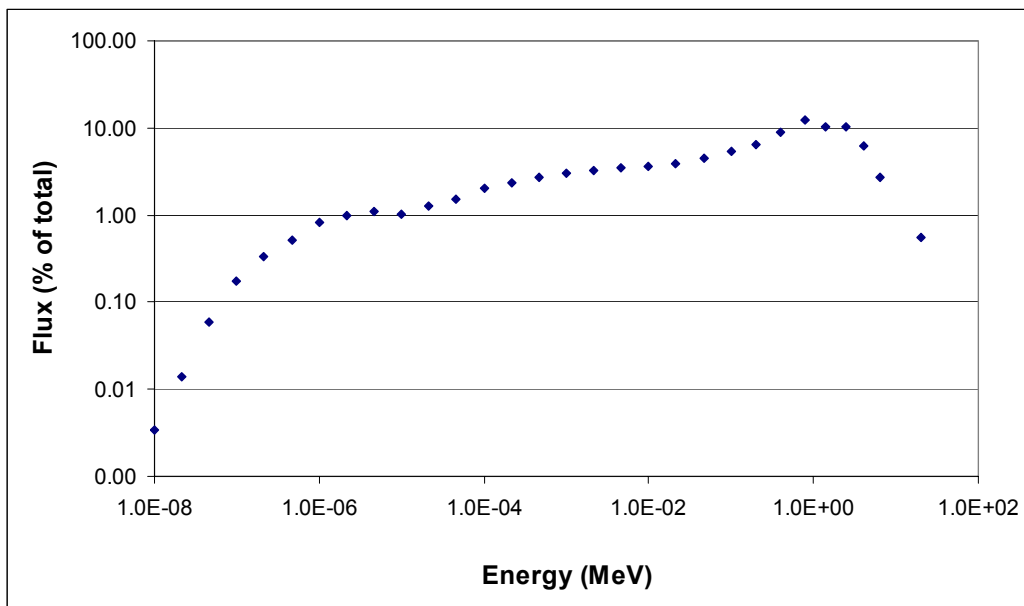

Figure I-2. Calculated Neutron Flux vs. Neutron Energy of Critical Limit Case

The following table (Table I-1) contains a list of the key parameters for the critical limit case. The information was extracted from the MCNP input and corresponding output file (*Fcwf1-tr*

and *Fcwf1-tr.out*, Attachment III). Note that although the range of parameters (ROP) is given for only the critical limit case, the results of the critical limit determination are applicable to all criticality calculations with a similar set of parameters.

Table I-1. Summary of Key Parameters for the Critical Limit Case

Category/ Description	Parameter	Values
Materials/ Fissionable Material	Fissionable Element	Uranium
	Physical Form	U oxides (schoepite – $UO_3:2H_2O$)
	Isotopic Composition	25.69 wt% ^{235}U in U
	Atomic density (atoms/b-cm)	^{235}U: 2.25 E-03
	Temperature	293 K
Materials/ Moderator	Element	Hydrogen
	Physical form	Water in hydrated compounds
	Atomic density (atoms/b-cm)	3.48E-02
	Ratio to fissile material (in region containing fissile material)	H/^{235}U: 15.4
	Temperature	293 K
Materials/ Reflector	Material/Physical form	Stainless steel; magma; tuff (concentric cylindrical layers and/or adjacent layers)
Materials/ Neutron Absorber	Element	Gd
	Physical form	$GdPO_4$
	Atomic density (atoms/b-cm)	6.32E-04
Geometry	Heterogeneity	Relatively homogeneous mixture of the degraded fuel with iron shot distributed within the empty spaces of the DOE canister
	Shape	Cylindrical
Neutron Energy	AENCF [a]	0.218 MeV
	EALF [a]	31.9 eV
	Neutron Flux Energy Spectra [a,b]	Thermal (T) = 1.9 % Intermediate (I) = 40.1 % Fast (F) = 58 %
	Fission Rate vs Neutron Energy [a,b]	Thermal (T) = 34.4 % Intermediate (I) = 53.7 % Fast (F) = 11.9%

NOTES: [a] Calculated in file *Fcwf1-tr_tallies.xls* (Attachment III)
[b] Spectral range defined as follows: thermal (T) [0-1 eV], intermediate (I) [1eV -100 keV], fast (F) [100 keV – 20 MeV]

I.2.2 Selecting Benchmark Experiments

The criticality experiments selected for the validation of the criticality calculation must be representative of the types of materials, conditions, and parameters to be examined in the calculation. A sufficient number of experiments with varying experimental parameters should be selected to ensure statistically significant results and a wide area of applicability. While there is no absolute guideline for the minimum number of critical experiments necessary to validate a model, the use of only a few (i.e., less than 10) experiments should be accompanied by a suitable technical basis supporting the rationale for acceptability of the validation results (Dean, J.C. and Tayloe, R.W., Jr. 2001 [DIRS 161786], page 5).

For the present application (igneous configuration containing degraded Enrico Fermi SNF), the criticality benchmark experiments were selected based on their fissile content, moderator, geometry and neutron spectrum. Other selection criteria included the presence of the neutron absorber (Gd) and reflector (containing Si as a scatterer). The benchmark experiments are from the *International Handbook of Evaluated Criticality Safety Benchmark Experiments* (NEA 2003 [DIRS 169530]) unless otherwise noted. The spectral characteristics were used as the initial criterion, and then the selections were further refined based on the majority of the parameters presented in Table I-1. The chosen set of criticality benchmark experiments was constructed to accommodate large variations in the range of parameters of the configurations and also to provide adequate statistics for the lower bound tolerance limit and critical limit calculations.

The selected benchmark experiments (a total of 93 individual cases) are presented in Table I-2 together with the published results of the MCNP code calculations. All cases were run using the neutron cross-section isotopic libraries described in (BSC 2003 [DIRS 164419], Table 5-3).

The experiments listed in Table I-2 are considered appropriate to represent the most reactive igneous configurations containing degraded Enrico Fermi SNF.

Table I-2. Critical Benchmark Experiments Selected for the Critical Limit Calculation

Experiment [a]	Case Name	Benchmark Values [a]		Calculated Values (MCNP) [b]		
		k_{eff}	σ_{exp}	k_{eff}	σ_{calc}	AENCF
Experiment IEU-COMP-THERM-001 (29 cases)	iect101	1.0000	0.004	0.9974	0.0009	0.21679
	iect102	1.0000	0.004	0.9960	0.0009	0.15817
	iect103	1.0000	0.004	0.9931	0.0010	0.10412
	iect104	1.0000	0.004	0.9974	0.0011	0.07405
	iect105	1.0000	0.004	1.0085	0.0009	0.04552
	iect106	1.0000	0.004	1.0003	0.0010	0.10793
	iect107	1.0000	0.004	0.9980	0.0010	0.11064
	iect108	1.0000	0.004	0.9960	0.0010	0.11867
	iect109	1.0000	0.004	1.0004	0.0008	0.1679
	iect110	1.0000	0.004	0.9967	0.0010	0.15756
	iect111	1.0000	0.004	0.9958	0.0010	0.15732
	iect112	1.0000	0.004	0.9964	0.0010	0.15568
	iect113	1.0000	0.004	0.9967	0.0010	0.0743
	iect114	1.0000	0.004	0.9979	0.0009	0.07375
	iect115	1.0000	0.004	0.9981	0.0010	0.074
	iect116	1.0000	0.004	1.0021	0.0009	0.05547
	iect117	1.0000	0.004	0.9965	0.0010	0.20814
	iect118	1.0000	0.004	0.9976	0.0011	0.13428
	iect119	1.0000	0.004	1.0045	0.0010	0.06114
	iect120	1.0000	0.004	1.0005	0.0009	0.15539

Table I-2 continued. Critical Benchmark Experiments Selected for the Critical Limit Calculation

Experiment [a]	Case Name	Benchmark Values [a]		Calculated Values (MCNP) [b]		
		k_{eff}	σ_{exp}	k_{eff}	σ_{calc}	AENCF
Experiment IEU-COMP-THERM-001 continued (29 cases)	iect121	1.0000	0.004	0.9988	0.0009	0.21334
	iect122	1.0000	0.004	0.9990	0.0011	0.19772
	iect123	1.0000	0.004	0.9952	0.0011	0.12826
	iect124a	1.0000	0.004	1.0004	0.0011	0.13305
	iect125	1.0000	0.004	0.9987	0.0009	0.05992
	iect126	1.0000	0.004	1.0044	0.0010	0.05663
	iect127	1.0000	0.004	1.0032	0.0009	0.05633
	iect128	1.0000	0.004	1.0051	0.0009	0.15824
	iect129	1.0000	0.004	1.0012	0.0010	0.15184
Experiment IEU-COMP-THERM-005 (2 cases selected) [c]	case2	0.980	0.003	0.9807	0.0004	0.48226
	case3	1.014	0.006	1.0158	0.0005	0.25976
Experiment IEU-COMP-THERM-002 (2 cases selected)	ieuct2_3	1.0017	0.0044	1.0026	0.0007	0.047
	ieuct2_4	1.0019	0.0044	1.0017	0.0007	0.049
Experiment HEU-COMP-THERM-004 (4 cases)	hct4-1	1.0000	0.0038	0.9876	0.0012	0.0744
	hct4-2	1.0000	0.0039	0.9889	0.0012	0.0736
	hct4-3	1.0000	0.0037	0.9916	0.0012	0.0756
	hct4-4	1.0000	0.0038	0.9912	0.0011	0.0742
Experiment HEU-MET-MIXED-005 (5 cases)	hmm5_1	1.0007	0.0027	1.01308	0.00057	0.307
	hmm5_2	1.0003	0.0028	1.0217	0.00055	0.247
	hmm5_3	1.0012	0.0029	1.01904	0.00052	0.212
	hmm5_4	1.0016	0.003	1.0145	0.0006	0.3175
	hmm5_5	1.0005	0.004	1.00682	0.00052	0.377
Experiment HEU-MET-THERM-001 (1 case) [c]	hmt001	1.0010	0.0060	1.0097	0.0010	0.0215
Experiment HEU-MET-THERM-014 (1 case) [c]	hmt14	0.9939	0.0015	1.0125	0.0004	0.0233
Experiment HEU-COMP-MIXED-001 (26 cases)	hcm-1	1.0000	0.0059	1.0027	0.001	0.1045
	hcm-2	1.0012	0.0059	1.0059	0.0011	0.1053
	hcm-5	0.9985	0.0056	0.9963	0.001	0.7833
	hcm-6	0.9953	0.0056	0.9899	0.001	0.7962
	hcm-7	0.9997	0.0038	0.9949	0.001	0.8015
	hcm-8	0.9984	0.0052	0.9915	0.0011	0.6872
	hcm-9	0.9983	0.0052	0.9931	0.0011	0.6536
	hcm-10	0.9979	0.0052	0.9941	0.001	0.6494
	hcm-11	0.9983	0.0052	0.9934	0.0011	0.6385
	hcm-12	0.9972	0.0052	0.9960	0.0011	0.6358
	hcm-13	1.0032	0.0053	0.9977	0.0011	0.6309
	hcm-15	1.0083	0.005	0.9949	0.0011	0.4671

Table I-2 continued. Critical Benchmark Experiments Selected for the Critical Limit Calculation

Experiment [a]	Case Name	Benchmark Values [a]		Calculated Values (MCNP) [b]		
		k_{eff}	σ_{exp}	k_{eff}	σ_{calc}	AENCF
Experiment HEU-COMP-MIXED-001 continued (26 cases)	hcm-16	1.0001	0.0046	0.9926	0.0011	0.4692
	hcm-17	0.9997	0.0046	1.0012	0.0011	0.4647
	hcm-18	1.0075	0.0046	1.0000	0.001	0.4625
	hcm-19	1.0039	0.0047	1.0000	0.0011	0.5191
	hcm-20	1.006	0.0065	1.0051	0.0015	0.5357
	hcm-21	1.0026	0.0064	1.0046	0.0016	0.5378
	hcm-22	1.0013	0.0064	0.9995	0.0016	0.5371
	hcm-23	0.9995	0.0053	1.0056	0.0015	0.535
	hcm-24	1.002	0.0053	1.0003	0.0016	0.5352
	hcm-25	0.9983	0.0053	0.9970	0.0014	0.5333
	hcm-26	0.9998	0.0053	1.0001	0.0015	0.5283
	hcm-27	0.9991	0.0053	0.9978	0.0016	0.5302
	hcm-28	1.0037	0.0053	1.0033	0.0015	0.541
	hcm-29	0.9992	0.0052	0.9998	0.0014	0.5401
Experiment HEU-COMP-MIXED-002 (23 cases)	hcm02_1	1.0000	0.0085	0.9866	0.0017	0.868
	hcm02_10	1.0000	0.0081	0.9856	0.0019	0.57
	hcm02_11	1.0000	0.0088	0.9829	0.0019	0.568
	hcm02_12	1.0000	0.0078	0.9900	0.0019	0.556
	hcm02_13	1.0000	0.0083	0.9874	0.0017	0.559
	hcm02_14	1.0000	0.0112	0.9880	0.0017	0.735
	hcm02_15	1.0000	0.0111	0.9850	0.0017	0.73
	hcm02_16	1.0000	0.0108	0.9861	0.0017	0.735
	hcm02_17	1.0000	0.0112	0.9861	0.0016	0.732
	hcm02_18	1.0000	0.0111	0.9902	0.0017	0.727
	hcm02_19	1.0000	0.0107	0.9910	0.0017	0.712
	hcm02_2	1.0000	0.0088	0.9907	0.0017	0.865
	hcm02_20	1.0000	0.0108	0.9824	0.0018	0.735
	hcm02_21	1.0000	0.0092	0.9843	0.0016	0.902
	hcm02_22	1.0000	0.009	0.9879	0.0019	0.899
	hcm02_23	1.0000	0.0093	0.9866	0.0016	0.896
	hcm02_3	1.0000	0.0093	0.9914	0.0016	0.724
	hcm02_4	1.0000	0.0087	0.9923	0.0017	0.716
	hcm02_5	1.0000	0.0089	0.9933	0.0017	0.722
	hcm02_6	1.0000	0.0093	0.9852	0.0018	0.574
	hcm02_7	1.0000	0.0086	0.9813	0.0019	0.578
	hcm02_8	1.0000	0.0068	0.9943	0.0018	0.537
	hcm02_9	1.0000	0.0076	0.9913	0.0018	0.541

NOTES: [a] Critical benchmark experiments are evaluated and benchmark values are given in (NEA 2003 [DIRS 169530]).
   [b] MCNP results are taken from (BSC 2003 [DIRS 164419], Attachment II) except where noted.
   [c] The results of the MCNP calculations for these cases are from (Moscalu, D.R. 2004 [DIRS 170909], Section 5.1.1).

I.3   ESTABLISHING THE RANGE OF APPLICABILITY

I.3.1   Range of Applicability of Benchmark Experiments

Table I-3, Table I-4, and Table I-5 summarize the range of applicability of the experiments listed in Table I-2. The information was partly excerpted from (BSC 2002 [DIRS 161781], Section 6.2), and information regarding the spectral characteristics of the experiments was added for the majority of the benchmarks from (NEA 2003 [DIRS 169530]).

Table I-3. Range of Applicability of Critical Benchmark Experiments, Part 1

Category/ Description	Parameter	Experiment IEU-COMP-THERM-001 (29 cases)	Experiment IEU-COMP-THERM-005 (2 cases selected)	Experiment IEU-COMP-THERM-002 (2 cases selected)
Materials/ Fissionable Material	Fissionable Element	Uranium	Uranium	Uranium
	Physical Form	UF_4 compound with polytetra-fluoroethylene	Mixture of UO_2 and Th metal	UO_2
	Isotopic Composition	29.83 wt% ^{235}U	36 wt% and 90 wt% ^{235}U	17 wt% ^{235}U
	Atomic density (atoms/b-cm)	^{235}U: 2.37E-03	^{235}U: 5.39E-03 and 1.35E-02	^{235}U: 1.89E-03
	Temperature	Room temp.	300 K	289 K and 424 K
Materials/ Moderator	Element	H; C	H; C	H
	Physical form	Polyethylene	Polyethylene	Water
	Atomic density (atoms/b-cm)	H: 7.52E-02 C: 3.92E-02	H: 7.2588E-02 C: 3.6294E-02	6.14E-02 and 6.68E-02
	Ratio to fissile material	$H/^{235}U$ = 4 to 222	$H/^{235}U$ = 1 and 10	Not calculated
	Temperature	Room temp.	300 K	289 K and 424 K
Materials/ Reflector	Material/Physical form	Unreflected or reflected by paraffin	K_{inf} experimental set-up	Reflected by water
Materials/ Neutron Absorber	Element	B, Cd, or none	None	Gd
	Physical form	Metallic sheets	N/A	Gd_2O_3 placed in rods
	Atomic density (atoms/b-cm)	Cd: 4.64E-02 ^{10}B: 3.21E-03	N/A	Gd: 2.16E-3
Geometry	Heterogeneity	Heterogeneous small cubes of fissile compound interspersed with moderator cubes	Heterogeneous set of stainless steel tubes forming a hexagonal infinite lattice	Cylindrical hexagonally pitched lattice of pins (pitch = 6.8 cm)
	Shape	Cuboid	Cylinder	Cylinder
Neutron Energy	AENCF	0.0455 to 0.2168 MeV	0.260 and 0.482 MeV	0.0470 and 0.0490 MeV
	EALF	0.11 to 9.09 eV	1E+02 and 2.97E+04 eV	Not available

Table I-3 continued. Range of Applicability of Critical Benchmark Experiments, Part 1

Category/ Description	Parameter	Experiment IEU-COMP-THERM-001 (29 cases)	Experiment IEU-COMP-THERM-005 (2 cases selected)	Experiment IEU-COMP-THERM-002 (2 cases selected)
Neutron Energy	Neutron Energy Spectra [a]	T: 1.8 to 22.8 % I: 24.9 to 40.2 % F: 49.6 to 63 %	T: 0 and 1.0 % I: 35.0 and 43.0 % F: 56.0 and 65.0 %	Not available
	Fission Rate vs Neutron Energy [a]	T: 49.9 to 90.9 % I: 7.1 to 42.8 % F: 2.0 to 11.1 %	T: 0.2 and 21.4 % I: 56.5 and 63.6 % F: 15 and 43.2 %	Not available

NOTE: [a] Spectral range defined as follows: thermal (T) [0-1 eV], intermediate (I) [1eV -100 keV], fast (F) [100 keV – 20 MeV]

Table I-4. Range of Applicability of Critical Benchmark Experiments, Part 2

Category/ Description	Parameter	Experiment HEU-COMP-THERM-004 (4 cases)	Experiment HEU-MET-MIXED-005 (5 cases)	Experiment HEU-MET-THERM-001 (1 case)
Materials/ Fissionable Material	Fissionable Element	Uranium	Uranium	Uranium
	Physical Form	UO_2 + Cu	U metal pellets	U metal foils
	Isotopic Composition	88.87 at% ^{235}U	89.39 wt% ^{235}U	93.23 wt% ^{235}U
	Atomic density (atoms/b-cm)	^{235}U: 5.13E-03	^{235}U: 4.24E-02	^{235}U: 3.84E-02 to 4.28E-02
	Temperature	293 K	Room Temp.	Room Temp.
Materials/ Moderator	Element	H	Si as scatterer H in sand	Si as scatterer H, C
	Physical form	Water	SiO_2 pellets interspersed with U pellets	Plates of polyethylene and silicon glass
	Atomic density (atoms/b-cm)	H: 6.67E-02	Si: 1.99E-02 H: 2.65E-05	H: 8.23E-02 - 8.28E-02 C: 4.11E-02 - 4.14E-02 Si: 2.17 - 2.24E-02
	Ratio to fissile material	H/^{235}U = 35	Not calculated	Not calculated
	Temperature	293 K	Room Temp.	Room Temp.
Materials/ Reflector	Material/ Physical form	Reflected by water and stainless steel	Reflected by polyethylene, SiO_2 sand and concrete	Reflected by polyethylene
Materials/ Neutron Absorber	Element	Gd; Sm	Boron	None
	Physical form	Gd_2O_3 or Sm_2O_3 rods	Impurity in SiO_2	N/A
	Atomic density (atoms/b-cm)	Gd: 3.11E-04	^{10}B: 4.40E-08	N/A
Geometry	Heterogeneity	Cylindrical hexagonally pitched double lattice of cross shaped fuel rods and absorber rods	Complex hexagonal geometry of pellets in Al tubes	Rectangular column of plates and foils

Table I-4 continued. Range of Applicability of Critical Benchmark Experiments, Part 2

Category/ Description	Parameter	Experiment HEU-COMP-THERM-004 (4 cases)	Experiment HEU-MET-MIXED-005 (5 cases)	Experiment HEU-MET-THERM-001 (1 case)
Geometry	Shape	Cylinder	Cylinder	Parallelepiped
Neutron Energy	AENCF	0.0736 - 0.0756 MeV	0.212 - 0.377 MeV	0.0212 MeV
	EALF	1.35 to 1.52 eV	1.48 to 5150 eV	0.0865 eV
	Neutron Energy Spectra [a]	T: 3.6 to 4.1% I: 38.2 to 38.5% F: 57.6 to 58.1%	T: 0.3 to 25.0 % I: 28.1 to 50.5 % F: 46.8 to 54.2 %	T: 22.7 % I: 27.7 % F: 49.7 %
	Fission Rate vs Neutron Energy [a]	T: 60.6 to 62.6% I: 32.9 to 34.7% F: 4.5 to 4.7%	T: 4.4 to 68.4 % I: 20.5 to 68.4 % F: 11.1 to 27.2 %	T: 91.2 % I: 7.7 % F: 1.2 %

NOTE: [a] Spectral range defined as follows: thermal (T) [0-1 eV], intermediate (I) [1eV -100 keV], fast (F) [100 keV – 20 MeV]

Table I-5. Range of Applicability of Critical Benchmark Experiments, Part 3

Category/ Description	Parameter	Experiment HEU-MET THERM-014 (1case)	Experiment HEU-COMP-MIXED-001 (26 cases)	Experiment HEU-COMP-MIXED-002 (23 cases)
Materials/ Fissionable Material	Fissionable Element	Uranium	Uranium	Uranium
	Physical Form	U metal foils	UO_2	UO_2
	Isotopic Composition	93.23 wt% ^{235}U	93.15 wt% ^{235}U	89.42 and 89.6 wt% ^{235}U
	Atomic density (atoms/b-cm)	^{235}U: 3.84E-02 to 4.38E-02	^{235}U: 4.48E-03 to 1.39E-02	^{235}U: 1.26E-02 and 1.32E-02
	Temperature	293 K	Room Temp.	Room Temp.
Materials/ Moderator	Element	H, C Si as scatterer	H	H and Deuterium (D)
	Physical form	Plates of polyethylene and silicon glass	Water, alcohol-water solution, Plexiglas	Water and heavy water
	Atomic density (atoms/b-cm)	H: 8.19E-02 - 8.34E-02 C: 4.10E-02 - 4.17E-02 Si: 2.20 - 2.28E-02	Fuel Region: H:2.16E-2 (7 cases) H: 5.68E-2 (Plexiglas) H: 6.24E-2 (alcohol-water)	H: 7.36E-03 - 6.67E-02 D: 0 - 5.91E-02
	Ratio to fissile material	H/X: Not available Si/^{235}U = 42	0 to 49	Not calculated
	Temperature	Room Temp.	Room Temp.	Room Temp.
Materials/ Reflector	Material/Physical form	Reflected by polyethylene	Reflected by polyethylene	Reflected by water stainless steel and concrete walls
Materials/ Neutron Absorber	Element	None	None	None
	Physical form	N/A	N/A	N/A

Table I-5. Range of Applicability of Critical Benchmark Experiments, Part 3

Category/ Description	Parameter	Experiment HEU-MET THERM-014 (1case)	Experiment HEU-COMP-MIXED-001 (26 cases)	Experiment HEU-COMP-MIXED-002 (23 cases)
Materials/ Neutron Absorber	Atomic density (atoms/b-cm)	N/A	N/A	N/A
Geometry	Heterogeneity	Rectangular column of plates and foils	Complex arrays of canisters in rectangular geometry	Hexagonal array of tubes containing UO_2 in a cylindrical tank
	Shape	Parallelepiped	Cylinder	Cylinder
Neutron Energy	AENCF	0.0234 MeV	0.1045-0.8015 MeV	0.537 – 0.899 MeV
	EALF	Not Available	0.438 to 2.14E+03	237 - 4.61E+04 eV
	Neutron Energy Spectra[a]	Not Available	T: 4.3 to 26.1 % I: 14.2 to 25.9 % F: 48.3 to 81.4 %	T: 0.4 – 8.0 % I: 16.0 – 33.8 % F:65.1 – 82.9 %
	Fission Rate vs Neutron Energy[a]	Not Available	T: 25.4 to 78.0 % I: 16.4 to 43.1 % F: 5.6 to 49.3 %	T: 3.8 – 34.5 % I: 26.8 – 54.6 % F: 31.9 – 63.6 %

NOTE: [a] Spectral range defined as follows: thermal (T) [0-1 eV], intermediate (I) [1eV -100 keV], fast (F) [100 keV – 20 MeV]

I.3.2   Comparing the Range of Applicability and Range of Parameters

The validation of the criticality calculation needs to show that the collective range of parameters of the benchmark critical experiments (Range of Applicability, or ROA) and the range of the evaluated parameters of the system (Range of Parameters, or ROP) are nearly identical. Since this is not usually practical for all parameters, it is acceptable to use critical benchmark experiments that cover most of the ROP of the system under evaluation as long as the parameters outside the range do not cause a trend in bias. For cases where a trend in bias is identified, the ROA can be extended, but a penalty on the critical limit determined for the subset of benchmark experiments needs to be evaluated and applied.

For the present analysis, the comparison between ROA and ROP was structured on the subset of benchmark experiments selected to cover the critical limit case. The ROP for the critical limit case (from Table I-1) was compared to the collective ROA of the selected benchmark experiments described in Table I-3, Table I-4, and Table I-5. The findings are presented in Table I-6.

The ROA for this set of experiments covers the ROP for all parameters that characterize the criticality limit case for the codisposal waste package containing Enrico Fermi SNF.

Table I-6 Range of Parameters vs. Range of Applicability

Category/ Description	Parameter	Range of Parameters (Calculation)	Collective Range of Applicability (Benchmarks)	Validation Comments
Materials/ Fissionable Material	Fissionable Element	Uranium	Uranium	Within range
	Physical Form	U oxides (schoepite – $UO_3:2H_2O$)	UF4; UO_2; U-metal	UO_3 expected to be similar to UO_2
	Isotopic Composition	25.69 wt% ^{235}U in U	17 to 93.23 wt% ^{235}U	Within range
	Atomic density (atoms/b-cm)	^{235}U: 2.25 E-03	^{235}U: 1.89E-03 to 4.28E-02	Within range
	Temperature	293 K	Room temperature and 424 K	Within range
Materials/ Moderator	Element	H	H, D, C Si as scatterer	Within range
	Physical form	Water in hydrated compounds	Water, polyethylene, Si	Within range
	Atomic density (atoms/b-cm)	H: 3.48E-02	H: 2.65E-05 to 8.34E-02	Within range
	Ratio to fissile material	H/^{235}U: 15.4	H/^{235}U: 0 to 222	Within range
	Temperature	293 K	Room temperature and 424 K	Within range
Materials/ Reflector	Material/ Physical form	Stainless steel; magma; tuff	No reflector, paraffin, water, steel, concrete, polyethylene, or sand	ROA reflectors cover the actual reflectors for the system
Materials/ Neutron Absorber	Element	Gd	Gd; Sm; B, Cd in one experiment	Within range
	Physical form	$GdPO_4$	Gd_2O_3	Within range
	Atomic density (atoms/b-cm)	6.32E-04	3.11E-04 to 2.16E-03	Within range
Geometry	Heterogeneity	Relatively homogeneous mixture	Homogeneous and heterogeneous configurations	Differences should not affect results [b]
	Shape	Cylindrical	Cylindrical, rectangular	Within range
Neutron Energy	AENCF	0.218 MeV	0.0212 to 0.902 MeV	Within range
	EALF	31.9 eV	0.0455 to 4.61E+04 eV	Within range
	Neutron Flux Energy Spectra [a]	T: 1.9 % I: 40.1 % F: 58 %	-T: 0 to 26.1 % -I: 14.2 to 50.5 % -F: 46.8 to 82.9 %	Within range
	Fission Rate vs Neutron Energy [a]	T: 34.4 % I: 53.7 % F: 11.9%	-T: 0.2 to 90.9 % -I: 7.1 to 68.4 % -F: 1.2 to 63.6 %	Within range

NOTES: [a] Spectral range defined as follows: thermal (T) [0-1 eV], intermediate (I) [1eV -100 keV], fast (F) [100 keV – 20 MeV]

[b] Geometry is not considered as important a parameter as material configurations when comparing ROA vs. ROP. (Dean, J.C. and Tayloe, R.W., Jr. 2001 [DIRS 161786], page 19)

I.4   ESTABLISHING THE LOWER BOUND TOLERANCE LIMIT

The lower bound tolerance limit serves as an important component of the critical limit (see Section I.5). Its purpose is to quantify the biases and uncertainties that cause the calculated results to deviate from the true value of k_{eff} for a critical experiment. A trend (that is, a linear correlation between the value of k_{eff} and the value of a spectral or physical parameter (YMP 2003 [DIRS 165505], Section 3.5.3.2.6)) is an indication of systematic errors or bias inherent in the calculational method used to estimate criticality. Any such errors or bias must be taken into account when setting the lower bound tolerance limit. In addition, uncertainties must be considered.

The methodology for calculating the lower bound tolerance limit is presented in Figure 3-6 of (YMP 2003 [DIRS 165505]). Regression–based methods are applied to identify possible trending of the calculated values of k_{eff} for all spectral and/or physical parameters. If trends are identified, then the LUTB method (YMP 2003 [DIRS 165505], Section 3.5.3.2.7) is used to calculate the lower bound tolerance limit for each trending parameter. The trending parameter that results in the most conservative (lowest) lower bound tolerance limit is then selected. If no significant trends in any parameter are identified, then random sample based methods are applied to calculate the lower bound tolerance limit.

Before applying the regression tests, an adjustment to the k_{eff} value calculated with MCNP (k_{calc}) was made as suggested in (Dean, J.C. and Tayloe, R.W., Jr. 2001 [DIRS 161786], p.8) for the critical benchmark experiments that were slightly super- or sub- critical. The MCNP calculated value (k_{calc}) was normalized to the experimental value (k_{exp}) using the following formula:

$$k_{norm} = k_{calc} / k_{exp} \qquad\qquad (1)$$

This normalization does not affect the inherent bias in the calculation due to very small differences in k_{eff}. Unless otherwise mentioned, the normalized k_{eff} values (k_{norm}) have been used in all subsequent calculations.

I.4.1   Evaluating Possible Trending

Each subset of normalized k_{eff} values was tested for trending against available spectral and/or physical parameters (e.g., average energy of a neutron causing fission [AENCF]) using a series of tests. Trending in this context is defined as linear regression of k_{eff} on the predictor variable(s). The linear regression fitted equation is in the form $y(x) = a + bx + \varepsilon$, where ε is the random error component (residuals). The trending was checked using well-established indicators or goodness-of-fit tests concerning the regression parameters.

The first test for trending was the regression analysis tool built in to the Microsoft Excel software. As a first indicator, the coefficient of determination (r^2) (Scheaffer, R.L. and McClave, J.T. 1990 [DIRS 154197], p. 390) can be used to evaluate the linear trending. The coefficient of determination, which is available as a result of using linear regression statistics, represents the proportion of the sum of squares of deviations of the y values about their mean that can be attributed to a linear relation between y and x.

Another test for the presence of linear trending was to check the goodness-of-fit against a null hypothesis on the slope (b) (Scheaffer, R.L. and McClave, J.T. 1990 [DIRS 154197], p. 382). The slope test requires calculating the test statistic T (Scheaffer, R.L. and McClave, J.T. 1990 [DIRS 154197], p. 382 and p. 371):

$$T = b\sqrt{\frac{(n-2)S_{xx}}{SS_E}} \tag{2}$$

where b is the slope of the fitted linear regression equation and

$$S_{xx} = S_{xx} = \sum_{i=1,n}(x_i - \bar{x})^2 \tag{3}$$

$$SS_E = \sum_{i=1,n}(y_i - a - bx_i)^2 \tag{4}$$

The test statistic T was then compared to the Student's t-distribution ($t_{\alpha/2,n-2}$) with 95% confidence and $n-2$ degrees of freedom (Scheaffer, R.L. and McClave, J.T. 1990 [DIRS 154197], p. 659), where n is the initial number of points in the subset. Given a null hypothesis of "no statistically significant trend exists (slope is zero)", the hypothesis was accepted if $|T| < t_{\alpha/2,n-2}$, and rejected otherwise. Unless the data is exceptional, the linear regression results will have a non-zero slope. By only accepting linear trends that the data supports with 95% confidence, trends due to the randomness of the data were eliminated. A good indicator of this statistical process is evaluation of the P-value probability (calculated by the regression tool in Excel) that gives a direct estimation of the probability of having a linear trending due only to chance.

The last test employed as part of the regression analysis was determining whether or not the final requirements of the simple linear regression model were satisfied (Scheaffer, R.L. and McClave, J.T. 1990 [DIRS 154197], p.377 and p.401). The error component (residuals) need to be normally distributed with mean zero, and also the residuals need to show a random scatter about the line y = 0 (no pattern). These requirements were verified for the present calculation using the built-in statistical functions in Excel and by applying an omnibus normality test (D'Agostino, R.B. and Stephens, M.A., eds. 1986 [DIRS 160320], p.372) on the residuals.

The results of the trending parameter analysis for the criticality benchmarks chosen in Section I.2.2 are presented in Table I-7 for the most conservative trending parameter. AENCF is the energy per source particle lost to fission divided by the weight per source neutron lost to fission from the "problem summary section" of the MCNP output.

Table I-7. Trending Parameter Results for the Criticality Benchmark Set

Trend Parameter	n	Intercept	Slope	r^2	T	$t_{0.025, n-2}$	P-value	Goodness-of-fit Tests	Valid Trend
AENCF [a]	93	1.0026	-0.0149	0.283	-5.997	1.9897 [b]	4.01E-8	Passed (partially)	Yes

NOTES: [a] All data calculated in file *Igneous_CL_Calc.xls* in Attachment III except as noted.
   [b] Value interpolated from (Natrella, M.G. 1963 [DIRS 103886], Table A-4).

The trending parameters for AENCF (r^2, T, P-value) from Table I-7 indicate a strong trend of k_{eff} with AENCF. However, the parameter data marginally fails the residual normality tests. Since the residuals fail the normality test by a small margin and the other trending parameters are so strong, the linear trend can be judged to be valid. The LUTB method (YMP 2003 [DIRS 165505], Section 3.5.3.2.7) is used to calculate the lower bound tolerance limit.

I.4.2 Calculating Lower Bound Tolerance Limit

The lower bound tolerance limit is calculated for this situation using the LUTB method implemented in the CLREG code [DIRS 159483]. The CLREG input, utility, and output files generated for this calculation (filenames *igneous.csv*, *igneous.utl*, and *igneousout.csv*, respectively) are included in Attachment III, subdirectory */Attach_I/*. Figure I-3 presents the k_{eff} values and the calculated lower bound tolerance limit for this set of benchmark experiments. The lower bound tolerance limit, f(AENCF), can be expressed using the following function (derived in file *Igneous_CL_Calc.xls* in Attachment III):

$$f(AENCF) = 0.96797 \text{ for } 0 \text{ MeV} < AENCF < 0.1679 \text{ MeV} \tag{5}$$

$$f(AENCF) = -1.3660\text{E-}02 * AENCF + 0.970271 \text{ for } 0.1679 \text{ MeV} \leq AENCF < 0.902 \text{ MeV} \tag{6}$$
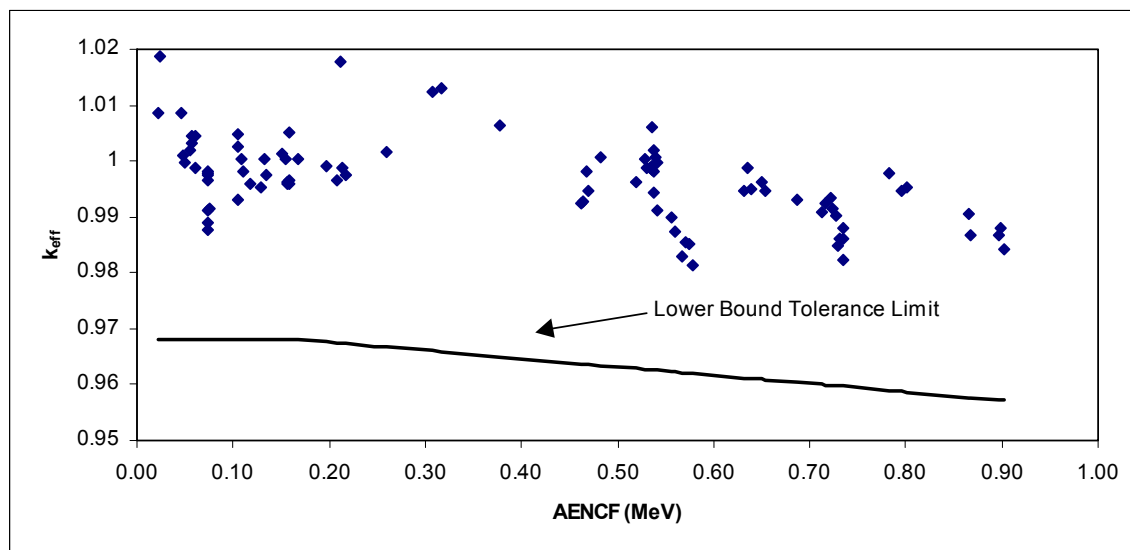

Figure I-3. Lower Bound Tolerance Limit for Criticality Benchmark Set

I.5 ESTABLISHING ADDITIONAL UNCERTAINTIES

An additional allowance (Δk_s) must be made (YMP 2003 [DIRS 165505], Section 3.5.3.2.10) for

(a) statistical or convergence uncertainties, or both in the computation of k_s

(b) material and fabrication tolerances, and

(c) uncertainties due to the geometric or material representations used in the computational method

The allowance for item (a) is quantified by the relative error in k_{eff} (σ) calculated by MCNP. For additional conservatism, this value was doubled. The allowances for items (b) and (c) are not considered in this calculation as the results are based on the inputs and representations presented throughout this analysis. Variations in geometric representation and material dimensions and compositions are not considered in this calculation, nor are they bounded by the results of this analysis, unless demonstrated. Thus the value of Δk_s is established as $\Delta k_s = 2\sigma$.

I.6 CALCULATION OF THE CRITICAL LIMIT

The critical limit equation (YMP 2003 [DIRS 165505], Section 3.5.3.2.5) is represented as follows:

$$CL(x) = f(x) - \Delta k_{EROA} - \Delta k_{ISO} - \Delta k_m \qquad (7)$$

where

$x =$ a neutronic parameter used for trending

$f(x) =$ the lower bound tolerance limit function accounting for biases and uncertainties that cause the calculation results to deviate from the true value of k_{eff} for a critical experiment, as reflected over an appropriate set of critical experiments

$\Delta k_{EROA} =$ penalty for extending the range of applicability

$\Delta k_{ISO} =$ penalty for isotopic composition bias and uncertainty

$\Delta k_m =$ an arbitrary margin to ensure subcriticality for preclosure and turns the CL function into an upper subcritical limit function (it is not applicable for use in postclosure analyses because there is no risk associated with a subcritical event)

The critical limit is associated with a specific type of configuration and is characterized by a representative set of benchmark criticality experiments. For the most reactive igneous configurations containing Enrico Fermi SNF and the associated set of benchmark criticality experiments, the above terms take the following values:

$f(x) =$ f(AENCF), determined in Section I.4.2 (Eq. 5 and 6) for AENCF between 0 and 0.902 MeV

$\Delta k_{EROA} =$ 0, since ROP is within the ROA

$\Delta k_{ISO} =$ 0, because no burnup is assumed for the fissile isotopes

$\Delta k_m =$ 0, since this is a postclosure analysis.

For the critical limit case analyzed in this calculation, the evaluated AENCF is 0.218 MeV. The critical limit can be calculated by replacing this value in the corresponding expression for f(AENCF) (Eq. 6):

$$CL = f(0.218) = -1.3660E\text{-}02 * 0.218 + 0.970271 = 0.9673$$

This critical limit must be further adjusted by the parameter for additional uncertainties (see Section I.5) by using the following equation for the criticality potential criterion (YMP 2003 [DIRS 165505], Section 3.5.3.2.10):

$$k_s + \Delta k_s < CL \tag{8}$$

where

$k_s =$ calculated k_{eff} for the system

$\Delta k_s =$ allowance for additional uncertainties (Section I.5)

$CL =$ critical limit, above

Using the values calculated above, it can be shown that igneous configurations with Fermi fuel are safely subcritical for:

$$k_s + 2\sigma < 0.9673 \tag{9}$$

ATTACHMENT II

Listing of Files Contained in Attachment III

This attachment contains a listing of the files contained on the attachment CD of this calculation (Attachment III). The zip archive was created using WINZIP 8.1. The CD was written using ROXIO Easy CD Creator 5 Basic installed on CRWMS M&O tag number 503009 central processing unit, and can be viewed on most standard CD-ROM drives. The files on the CD are as listed in the table below. Additional information is given in Table II-1.

Table II-1. File Listing and Description of CD

File Name	File Size (bytes)	File Date	File Time	Description
Root Directory \				
ATR.xls	60,416	09/28/2006	11:34a	Excel spreadsheet containing dimensions and material data for ATR intact and degraded cases
Fermi.xls	225,280	09/28/2006	01:55p	Excel spreadsheet containing dimensions and material data for Fermi intact and degraded cases
FFTF.xls	36,352	09/28/2006	11:39a	Excel spreadsheet containing dimensions and material data for FFTF intact and degraded cases
FSV.xls	15,360	09/27/2006	09:57a	Excel spreadsheet containing dimensions and material data for FSV intact cases
materials.xls	123,904	09/28/2006	02:17p	Excel spreadsheet containing dimensions and material data for HLW glass, magma, tuff, and structural materials
MCNP_files.zip	21,435,149	09/18/2006	03:24p	Archive file containing MCNP input and output files (see explanation below)
TMI.xls	20,480	09/28/2006	11:42a	Excel spreadsheet containing dimensions and material data for TMI intact and degraded cases
TRIGA.xls	146,432	09/28/2006	11:44a	Excel spreadsheet containing dimensions and material data for TRIGA intact and degraded cases
Shippingport.xls	20,992	09/27/2006	12:33p	Excel spreadsheet containing fuel compositon calculations for Shippingport PWR and LWBR intact cases
Subdirectory \Attach_I				
Fcwf1-tr	19,051	7/14/2004	09:06a	MCNP input file for critical limit calculation
Fcwf1-tr.out	486,851	7/14/2004	09:06a	MCNP output file for critical limit calculation
Fcwf1-tr_tallies.xls	45,056	7/26/2004	05:22p	Excel file summarizing MCNP output
igneous.csv	2,613	7/6/2004	01:33p	CLREG input file for calculating lower bound tolerance limit

Table II-1 continued. File Listing and Description of CD

File Name	File Size (bytes)	File Date	File Time	Description
Subdirectory \Attach_I				
igneous.utl	5,270	7/6/2004	01:34p	CLREG utility file for calculating lower bound tolerance limit
igneousout.csv	7,893	7/6/2004	01:34p	CLREG output file for calculating lower bound tolerance limit
Igneous_CL_Calc.xls	192,512	8/27/2004	08:40a	Excel file evaluating normality of data and generating CLREG input file

The Excel spreadsheets (filenames *.xls*) contain all calculations performed for this document.

The archive file *MCNP_files.zip* contains 296 total files (not including folders). Files with names that do not end in "o" are MCNP input files, and files with names that end in "o" are MCNP output files. When the files are extracted, a directory structure is generated as follows:

/1_N-reactor/ - Contains files for the cases listed in Tables 7.1-1 and 7.1-2.

/2_fftf/ - Contains files for the cases listed in Tables 6.4-2, 7.2-1, 7.2-2, and 7.2-3.

/3_Fermi/ - Contains files for the cases listed in Tables 7.3-1, 7.3-2, and 7.3-3.

/4_ShipPWR/ - Contains files for the cases listed in Tables 7.4-1 and 7.4-2.

/5_ShipLWBR/ - Contains files for the cases listed in Tables 7.5-1 and 7.5-2.

/6_fsv/ - Contains files for the cases listed in Tables 7.6-1 and 7.6-2.

/7_triga/ - Contains files for the cases listed in Tables 7.7-1, 7.7-2, and 7.7-3.

/8_atr/ - Contains files for the cases listed in Tables 7.8-1, 7.8-2, and 7.8-3.

/9_tmi/ - Contains files for the cases listed in Tables 7.9-1, 7.9-2, and 7.9-3.

Within these subdirectories, the file naming system is as follows:

#.W.xxx.yy.z#

where

# = digit from 1 to 9 to denote SNF fuel type in the model.
W = capital letter denoting the calculation set (i.e. calculation set A is damage scenarios, B is drift scenarios, C is degradation scenarios).
xxx = three-character code to denote damage scenario. The first character is either w (waste package barrier present) or x (waste package barrier absent and replaced by magma). The second character is i (intact, no slump), p (partial slump), or c (complete slump). The third character is either g (HLW glass present) or x (glass absent and replaced by magma).

yy   = two-character code to denote drift scenario. The first character is either h (hot magma) or c (cooled magma). The second character is either d (dry magma) or w (wet magma, seepage returned).

z#   = two-character code to denote degradation scenario. The first character is f for flowthrough conditions or b for bathtub conditions. The second character is a digit to denote the degradation configuration where 0 is non-degraded, 1 is only fuel degraded (metals non-degraded), 2 is only metal degraded (fuel non-degraded), and 3 is both fuel and metal degraded

Note that as per Section 6.4.3, there is a ninth case in calculation set C to evaluate the effects of degrading the HLW glass into clay. The 'z#' component is there replaced with a 'v'. Also, the cases for calculation set C presented in Table 6.4-2 has an 'H' for the 'W' component (instead of a 'C'), which represents hematite cases.